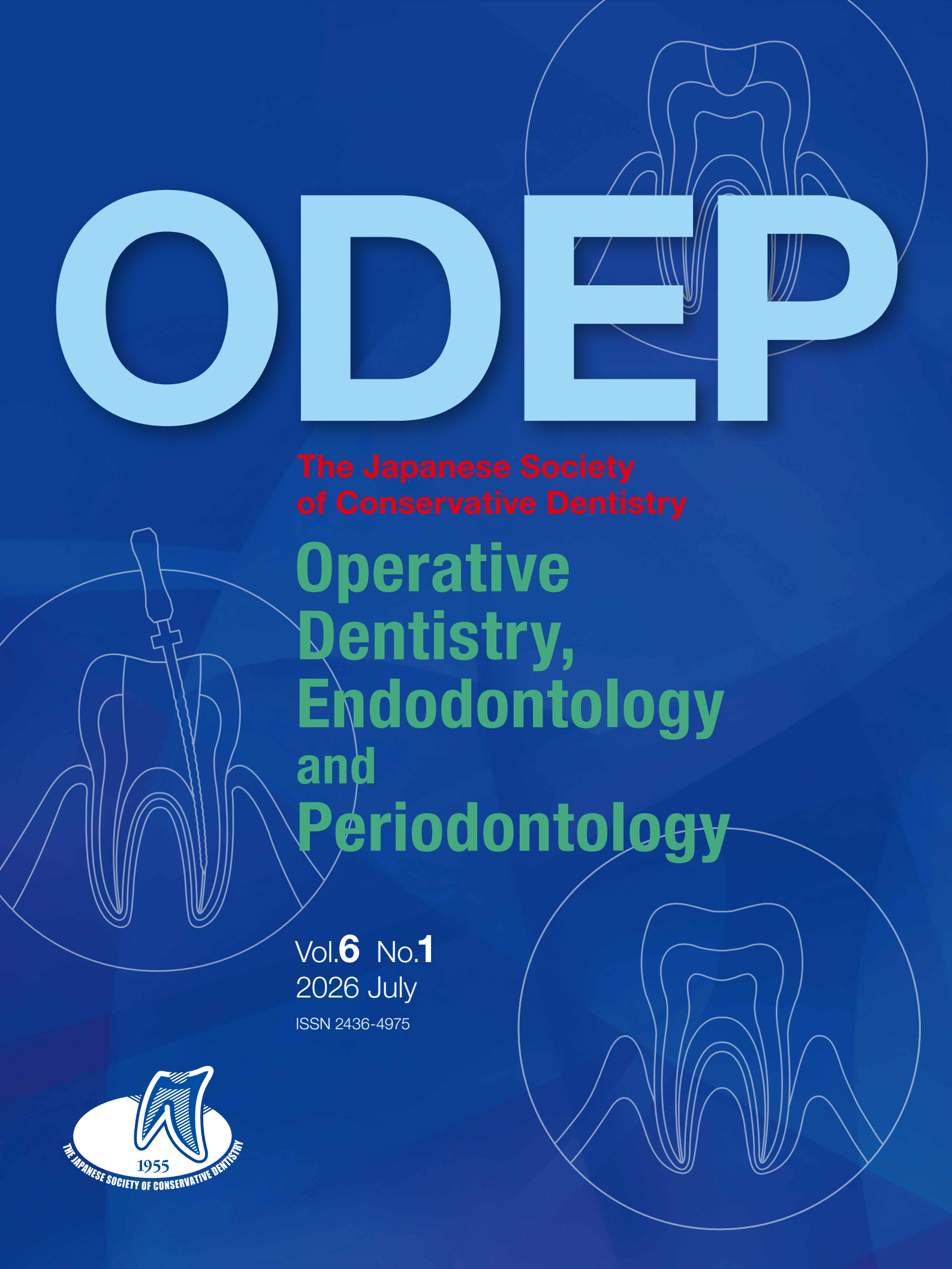

ODEP

The Japanese Society of Conservative Dentistry

Operative Dentistry, Endodontology and Periodontology

Vol.6 No.1
2026 July
ISSN 2436-4975

1955
THE JAPANESE SOCIETY OF CONSERVATIVE DENTISTRY

HySolate SyntX
ハイソレート　シンテックス

ポリイソプレンエラストマー製ノンラテックス印字済みデンタルダム
NaOCl(3%,6%)、EDTA等の薬液への耐性あり

READY.SET.PLACE

- ✓ 超時短、高い伸縮性と引張強度
- ✓ 高い視認性 と写真映え
  （ハイコントラスト ブルー）
- ✓ テンプレート印字とロゴの位置で、
  複雑な症例でも
  位置確認・操作が簡単！

NEWアイテム

Ready to Punch
Dam-It, It`s Easy

ノンラテックス・ブルー　印字済み

ラバーダムの定義をさらに変える

KENDA

シリコンポリッシャー

- コンポジットレジン用
- すべてのジルコニア・セラミック類用
- すべてのメタル類用

コンポジットをスピーディーに
ジルコニアやチタンに確実なツヤを

1. スイス製で1本250円から
2. 研磨ペースト不要
3. シリコン印象材メーカーから
   生まれたシリコンポリッシャー
4. 滅菌可能

@COLTENE.JP

FOLLOW US

お問い合わせ　コルテンジャパン合同会社　042-595-6945

販売名：シリコーンポリッシャー　届出番号：13B1X10231000133
販売名：ラテックスフリー　ラバーダム　届出番号：13B1X10231000251

COLTENE

NEO DENTAL CHEMICAL PRODUCTS CO., LTD.

RENEW

素材の品質も 性能の一部です。

1本で覆髄から裏層まで！

DirectCapping+BaseLiner CAVIOS with MTA

トドイテ タレナイ

新黒Sチップ 標準添付

MTA成分「ネオホワイトピュア®」を配合したスムーズで切れの良い、歯質へのなじみが高い直接覆髄裏層材です。MTAの効果発現を促す処方により光重合裏層材としての理工学的性質に加え、直接覆髄材としての性能を有します。
1本で覆髄にも裏層にも使える２in１製材です。
従来のMサイズチップに代わり新たにＳサイズ遮光チップを標準添付しました。
微細な部分への到達性が高まっただけでなく、適応量がより細かくコントロール可能となり、同時にペーストの垂れも低減されました。

光重合 覆髄+裏層材

D-Cavios® MTA

ネオホワイトピュア® 配合

1.5g入シリンジ　1本
先端チップ　15本 **(Sサイズ)**
標準価格 6,500円

補充用　ネオ ブラックチップ(S)　30本　NEW
一般医療機器
医療機器届出番号　13B1X00154000013　標準価格 2,000円

※従来のMサイズは単品でお求めいただけます。

覆髄+裏層 2in1
D-キャビオス®MTA

医療機器認証番号　304ADBZX00054000
歯科用覆髄材料（歯科裏層用高分子系材料）
管理医療機器

製造販売業者
ネオ製薬工業株式会社
〒150-0012　東京都渋谷区広尾3丁目1番3号
Tel. 03-3400-3768（代）　Fax. 03-3499-0613

LA2507

GC友の会70周年記念

第6回国際歯科シンポジウム

東京国際フォーラム（東京都千代田区丸の内3-5-1）

2026.10.3 SAT ▷ 4 SUN

英知の結集

80億人の笑顔を育む歯科医療

Gather Knowledge, Create “8 billion” Smiles!

大変お得な
早割申込
受付中

THE 6TH INTERNATIONAL DENTAL SYMPOSIUM

65セッション

200名を超える登壇講師

※2026年6月現在

instagram

NISHIKA

Bioceramic material

バイオセラミックスが
封鎖性と生体親和性を向上

根管充填シーラとして

充填法
- シングルポイント法 *
- 側方加圧法
- 垂直加圧法

誰が練っても
いつも同じ仕上がり

歯科用覆髄材料・
歯科用根管充填シーラ

ニシカキャナルシーラー® BGmulti

覆髄材として

ペーストにパウダーを
混ぜると覆髄にも
使いやすい性状に。

[包装・標準価格]
ペースト：1本［A材 4.5g(2.5mL)、B材4.5g(2.5mL)］・13,000円／パウダー：1個［2g］・10,200円／
セット：ペースト1本、パウダー1個・22,000円

管理医療機器 一般的名称：歯科用覆髄材料・歯科用根管充填シーラ　医療機器認証番号：302ADBZX00055000　製造販売元：日本歯科薬品株式会社

＊シングルポイント根管充填用ツール「BGフィル」を販売しています。詳しくは、特設サイトをご覧ください。

【特設サイト】

NISHIKA 日本歯科薬品株式会社
本　社 山口県下関市竹崎町4-7-24 〒750-0025
営業所 大阪・東京・福岡
https://www.nishika.co.jp/
お問合せ・資料請求《お客様窓口》
0120-8020-96

そのホワイトスポット，低侵襲で治せます！

ホワイトスポット

指宿隆秀・品川淳一・保坂啓一 著

■ A4判／186頁／カラー
■ 定価 14,850円（本体 13,500円+税10%）
■ ISBN978-4-263-44772-7
■ 注文コード：447720

詳しい内容は
二次元コードの
リンク先から！

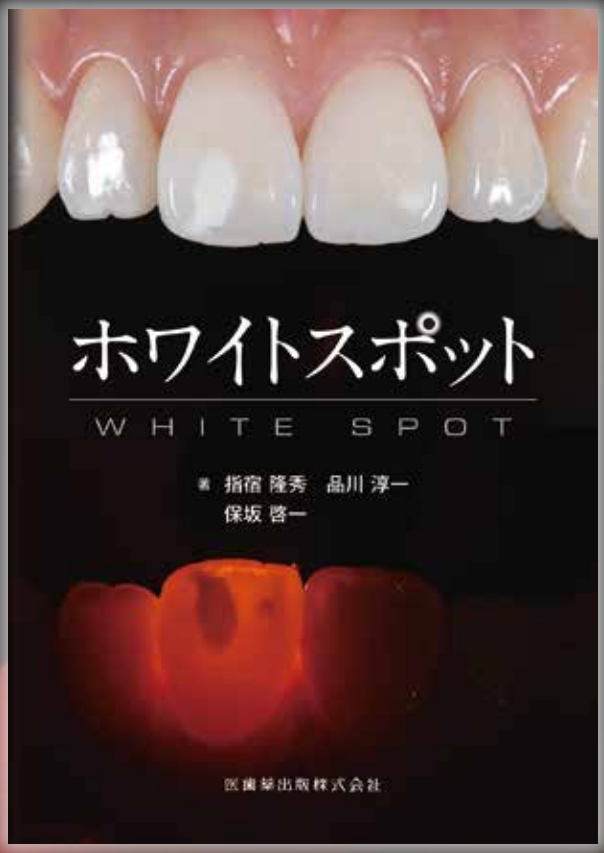

●ホワイトスポット（白斑）による審美障害に悩んでいるものの，「できるだけ歯を削りたくない」と治療に二の足を踏んでいる患者は少なくありません．

●近年，低粘性レジン浸潤法や深部レジン浸潤法などのホワイトスポット治療が確立されたことで，現在では低侵襲にて高い審美性を回復させることが可能になっています．

●本書は，ホワイトスポット治療の第一人者が使用器材から臨床の勘所までを豊富な臨床例とともに解説した必携の一冊です．

医歯薬出版株式会社 〒113-8612 東京都文京区本駒込1-7-10 TEL03-5395-7630 FAX03-5395-7633 https://www.ishiyaku.co.jp/

OPERATIVE DENTISTRY, ENDODONTOLOGY AND PERIODONTOLOGY

Vol. 6, No. 1 JULY 2026

CONTENTS

Published
by
THE JAPANESE SOCIETY OF CONSERVATIVE DENTISTRY (JSCD)
c/o Oral Health Association of Japan (Kōkūhoken kyōkai)
1-43-9, Komagome, Toshima-ku, Tokyo 170-0003
Japan

Editorial Board of Operative Dentistry, Endodontology and Periodontology (2026)

Original Article

ODEP 6 (1) : 1〜13, 2026

Development of a New Root Canal Sealer Using Zinc Oxide, Eugenol, and Oleic Acid

Munehiro MAEDA, Shuichi HASHIMOTO*, Taro NISHIDA,
Katsumi ISHITSUKA and Ichiroh KATSUUMI

Department of Endodontics, The Nippon Dental University School of Life Dentistry at Tokyo
*The Nippon Dental University

Abstract

Purpose: Eugenol, found in zinc oxide eugenol (ZOE), a commonly used root canal sealer, has antibacterial properties. However, eugenol can irritate tissues when used in high concentrations. A new ZOE sealer was developed by diluting eugenol with oleic acid to reduce the harmful effects of eugenol, which is released after filling, on periapical tissues. This study aimed to investigate the physical properties and antibacterial effects of this new ZOE sealer.

Methods: Tests were conducted on the hardening time, flow behavior, radiopacity, solubility, and sealing ability of this new ZOE sealer in accordance with International Organization for Standard (ISO) 6876, and these values were compared with a commonly used control ZOE sealer(Canals). Further, tests related to the clinical application of this sealer were conducted, including a size change test, a test of time-dependent changes in hardness of the sealer immersed in water, a bacterial growth prevention test using three types of bacteria, and a test of sealer effects on curing for two types of composite resins.

Results: The new ZOE sealer met the requirements of ISO 6876 for all test results except radiopacity. Setting time was shorter for the new ZOE sealer than for the control ZOE sealer, and was within 30 minutes. Viscosity was lower for the new sealer than for the control sealer. Disintegration ratios showed no significant difference between sealers. Unlike the control sealer, the new sealer did not show any dye penetration. The volume of the new sealer, unlike the control sealer, showed a tendency to continuously increase from 7 to 30 days after mixing. No significant difference in hardness was seen between the new and control sealers. Although the amount of eugenol in the new sealer was one-fifth that of the control sealer, antibacterial effects against *Prevotella intermedia* and *Porphyromonas gingivalis* were similar to those of the control sealer. The new sealer did not cause any significant change in the curing of composite resins, whereas the control sealer significantly inhibited curing.

Conclusion: The new ZOE sealer, developed by reducing the eugenol content of the sealer to approximately 30% using oleic acid and isostearic acid, is clinically applicable because it expands and cures gently, retains antibacterial properties, and does not inhibit the curing of composite resins.

Key words: new root canal sealer, ZOE sealer containing oleic acid, physical property of sealer

Corresponding author: Munehiro MAEDA, Department of Endodontics, The Nippon Dental University School of Life Dentistry at Tokyo, 1-9-20, Fujimi, Chiyoda-ku, Tokyo 102-8159, Japan
TEL: +81-3-3261-5698, FAX: +81-3-3264-8399, E-mail: maeda-mu@tky.ndu.ac.jp
Received for Publication: November 25, 2025/Accepted for Publication: February 12, 2026
DOI: 10.11471/odep.2026-001

Introduction

The eugenol in zinc oxide eugenol (ZOE), a commonly used root canal sealer, has anti-inflammatory, analgesic, and antibacterial properties[1,2]. However, at high concentrations, eugenol also exhibits tissue irritant effects[3,4], leading to issues such as inhibition of resin polymerization[5,6]. One reason why eugenol derived from ZOE can damage dental pulp and periapical tissues is that, after mixing zinc oxide and eugenol, the eugenol that is not chelated with zinc oxide is released from the hardened material.

Our research group has conducted detailed studies on changes to the content of physiologically active substances and the number of inflammatory cells in dental pulp when experimental dental pulp inflammation is induced by cavity formation in rat mandibular incisors. In addition, we have demonstrated that filling the cavity with a ZOE cement containing a standard amount of eugenol significantly suppresses the production of histamine and arachidonic acid metabolites in inflamed dental pulp tissue[7–9].

On the other hand, high concentrations of eugenol can cause significant irritation and cytotoxic effects on tissues[10–13]. Researchers are therefore developing root canal-filling cements that use unsaturated fatty acids as an alternative to eugenol[14]. Based on such reports, we diluted eugenol with oleic acid to minimize the tissue-damaging effects of excessive eugenol in ZOE sealer. This resulted in the creation of a new root canal ZOE sealer that is less irritating to periapical periodontal tissues compared to a conventional root canal ZOE sealer (Canals; GC SHOWAYAKUHIN Co., Tokyo, Japan).

Ishitsuka et al.[15] conducted *in vitro* experiments using cultured osteoblasts and rat dental pulp cells to clarify the concentration of eugenol exerting pharmacological effects versus that resulting in harmful effects. Consequently, they demonstrated that concentrations below 10^{-4} M have little effect on the proliferation of cultured cells, while concentrations above 10^{-3} M lead to slight inhibition of both cell proliferation and expression of alkaline phosphatase (ALP)[16–18].

Based on these results, this study aimed to develop a root canal ZOE sealer using a low concentration of eugenol diluted with oleic acid and to investigate various characteristics of the sealer, as well as its effectiveness against bacteria.

Materials and Methods

1. Composition of sealers

The new root canal ZOE sealer (hereafter referred to as "new ZOE sealer") was prepared by mixing the following powder with liquid at a ratio of 1 g to 0.5 mL. The powder composition included 400 mg zinc oxide (FUJIFILM Wako Pure Chemical, Osaka, Japan), 400 mg rosin (FUJIFILM Wako Pure Chemical), and 200 mg barium sulfate (FUJIFILM Wako Pure Chemical). The liquid composition consisted of 0.75 mL oleic acid (FUJIFILM Wako Pure Chemical), 0.10 mL isostearic acid (FUJIFILM Wako Pure Chemical), and 0.15 mL eugenol (Sigma-Aldrich, Tokyo, Japan). Accordingly, the eugenol content of the new ZOE sealer, which was prepared from a mixture of 1 g of powder and 0.5 mL of liquid, was equivalent to 0.075 mL. We filed a patent for the basic composition of the new ZOE sealer used in this experiment in October 2008, and the application was accepted as a patent (P5280801) in September 2013[19].

As the control root canal ZOE sealer (hereafter referred to as "control ZOE sealer"), we used the Canals conventional ZOE sealer. The control ZOE sealer was prepared by mixing the following powder and liquid at a ratio of 1 g to 0.3 mL. The powder composition included 400 mg zinc oxide, 400 mg rosin, 100 mg barium sulfate, and 100 mg bismuth subcarbonate[20]. The liquid composition consisted of 0.83 mL of eugenol and 0.17 mL of peanut oil. The eugenol content of the control ZOE sealer, made from a mixture of 1 g of powder and 0.3 mL of liquid, was equivalent to 0.249 mL. The eugenol content of the new ZOE sealer was therefore 30.12% of that of the control ZOE sealer, as calculated using the formula: (0.075 mL/0.249 mL) × 100%.

2. Hardening time of sealers

Teflon molds with an internal diameter of 10 mm and a thickness of 2 mm were prepared. Each mold was filled with the new ZOE sealer or control ZOE sealer. To measure the hardening times (in minutes) of the new ZOE sealer and control ZOE sealer, a Gilmore needle (1/4 lb; JAPAN MECC Co., Tokyo, Japan) with a flat end (1 mm diameter) was repeatedly lowered onto

Table 1 Hardening time of sealers

	Curing time
New ZOE sealer	23.0±1.0*
Control ZOE sealer	1,245.6±9.5

min; mean±SD, n=5, *：p<0.05

Curing times (in minutes) of the new ZOE sealer and control ZOE sealer were measured using a Gilmore needle at 37℃ and 100% humidity. This test was repeated five times for each sealer. Values in the table represent the mean±standard deviation (SD).

the surface of each sealer at 37℃ and 100% humidity. This test was repeated five times for each sealer (Table 1).

3. Flow behavior test of sealers

Immediately after mixing, 0.05 mL of each sealer was placed at the center of a glass plate measuring 40×40×5 mm. Then, 180 s after the mixing started, another glass plate of the same size was placed on top of the samples at room temperature, and a weight was added. The total weight, including the glass, was 120 g. Ten minutes after mixing began, the weight was removed. Maximum and minimum extension lengths (in millimeters) of the compressed sealer were measured, using the average to determine viscosity flow behavior. This test was conducted five times for each sealer (Table 2).

4. Radiopacity of sealers

The new ZOE sealer or control ZOE sealer was placed into a stainless-steel ring with an internal diameter of 10 mm and a depth of 1 mm. The sample was then placed on a glass plate and kept at 37℃ and 100% humidity for 24 h. These samples and an aluminum step wedge (with 1-mm steps) were placed directly on a photostimulable phosphor plate (YCR DT-1; DENTAL MFG Co., Tokyo, Japan). Radiographs were taken using an X-ray unit (Heliodent DS; Dentsply Sirona Inc., Bensheim, Germany) that operated at 60 kV and 7 mA for 0.2 s, with a focus-to-target distance of 30 cm. These were scanned using a phosphor plate scanner (Array arcana, AC 100 V, scan time, 30 s; Array Corp., Tokyo, Japan). After importing the digitized radiographs into Image J software (version 1.53; National Institutes of Health, Bethesda, MD, USA), mean gray-scale values of the sealer sample and aluminum step wedge were compared. Radiopacity was expressed as the equivalent thickness (in millimeters) of aluminum. This test was repeated five times for each sealer (Table 3).

Table 2 Flow behavior test of sealers

	Extension length
New ZOE sealer	22.26±0.47*
Control ZOE sealer	39.73±1.44

mm; mean±SD, n=5, *：p<0.05

Maximum and minimum extension lengths (in millimeters) of both the new ZOE sealer and the control ZOE sealer were measured when the sealer was compressed and stretched at room temperature. The average of these measurements was used to determine viscosity flow behavior. This test was conducted five times for each sealer.

Table 3 Radiopacity of sealers

	Radiopacity
New ZOE sealer	2.6±0.2*
Control ZOE sealer	3.8±0.5

Equivalent aluminum thickness: mm; mean±SD, n=5, *：p<0.05

The new ZOE sealer and control ZOE sealer were cured at 37℃ and 100% humidity for 24 h. Radiographs of these sealers and an aluminum step wedge were taken using the X-ray unit. After analyzing digitized radiographs using Image J software (version 1.53), mean gray-scale values for the sealer sample and aluminum step wedge were compared. Radiopacity is expressed as the equivalent thickness (in millimeters) of the aluminum used for comparison. This test was repeated five times for each sealer.

5. Solubility of sealers

After preparation, the new ZOE sealer or control ZOE sealer was immediately filled into a silicone tube with an inner diameter of 6 mm and a length of 5 mm, then cured at 37℃ with 100% humidity for 24 h. Before conducting the collapse test, the weight of each sealer was measured. Samples were then immersed in 50 mL of distilled water at 37℃ for 24 h. After soaking, the 50 mL of water was evaporated and removed, and the amounts of residual substances that collapsed and detached from the sample into the water were measured.

Table 4 Solubility of sealers

	Degradation rate
New ZOE sealer	0.75±0.19
Control ZOE sealer	0.55±0.12

%; mean±SD, n=5, p：>0.05

The new ZOE sealer and control ZOE sealer were cured at 37℃ with 100% humidity for 24 h, then immersed in distilled water at 37℃ for 24 h. The percentage of residual substance that collapsed and detached from each sealer was calculated using the following formula:(weight of residual substance/weight of sealer)×100 (%). This value was referred to as the degradation rate. This test was repeated five times for each sealer.

Table 5 Sealing ability of sealers

	Dye penetration length
New ZOE sealer	0*
Control ZOE sealer	19.40±0.89

mm; mean±SD, n=5, *：p<0.05

The new ZOE sealer or control ZOE sealer was filled into glass tubes after mixing the powder and liquid. The glass tubes, sealed with the sealer, were immersed in a 1% solution of methylene blue. The penetration length of methylene blue into each glass tube was measured after samples were left in the dye solution at 37℃ for 24 h. This test was conducted five times for each sealer.

The percentage of residual substances that collapsed and detached from each sealer was calculated using the following formula:(weight of residual substances/weight of sealer)×100 (%). This value was referred to as the degradation rate for the sealer. This test was repeated five times for each sealer (Table 4).

6. Sealing ability of sealers

The new ZOE sealer or control ZOE sealer was placed into glass tubes with an internal diameter of 5 mm and a length of 40 mm. These tubes were then filled to a depth of 20 mm. Immediately thereafter, the glass tubes sealed with the sealer were immersed in 1% methylene blue solution (FUJIFILM Wako Pure Chemical) at 37℃. After 24 h, penetration of methylene blue into each glass tube was measured. This test was repeated five times for each sealer (Table 5).

7. Size change of sealers

The change in size of the new ZOE sealer or control ZOE sealer was determined using the method described in Section 7.6 of the International Organization for Standardization (ISO) 6876[21]. A cylindrical container made of stainless steel (JAPAN MECC, Japan) with a diameter of 6 mm and a height of 12 mm, was filled with the sealer, covered with a glass plate, and stored for 24 h at 100% relative humidity and 37℃. The container filled with each sealer was immersed in distilled water at 37℃ for 1, 2, 5, 7, 9, 15, 20, and 30 days. After immersion, the thickness (in millimeters) of the sealer tablet was measured using a micrometer (MDC-25 MJ; Mitutoyo Co., Kanagawa, Japan). This test was repeated five times for each sealer (Fig. 1).

8. Hardness of sealers

To measure the hardness of the new ZOE sealer and control ZOE sealer, each sealer was placed in a glass tube (inner diameter, 8 mm; height, 5 mm), covered with a glass plate, and stored at 100% relative humidity and 37℃ for 24 h. The cured sealer was then immersed in distilled water at 37℃ for 1, 3, 6, 7, 10, 14, 21, 25, and 30 days. In contrast, the cured control sealer tablets were immersed in distilled water at 37℃ for only 1 and 7 days. The hardness of these sealer tablets was measured.

The hardness of sealers was measured as described by Ogura and Katsuumi[22]. Sealer tablets were placed on the test table of a texture analyzer (EZ Test; Shimadzu Co., Kyoto, Japan). A needle with a flat end (diameter, 1 mm) was vertically inserted into the center of the sealers at a speed of 1 mm/s. The degree of cure of the sealer was recorded using data processing software (Trapezium; Shimadzu Co.), expressed in units of Newtons (hereafter referred to as N). This test was repeated three times for each sealer (Fig. 2).

9. Preventing bacterial growth with sealers

The bacteria used in this study were *Prevotella intermedia* (*Pi*), *Porphyromonas gingivalis* (*Pg*), and *Enterococcus faecalis* (*Ef*). *Pi* and *Pg* were inoculated onto Anaero Columbia agar with rabbit blood (Japan Becton Dickinson Co., Tokyo, Japan), adjusted to a McFarland turbidity of 0.5 using a sterilized cotton swab. *Ef* was inoculated onto sheep blood agar (EIKEN CHEMICAL Co., Tokyo, Japan) and adjusted to a McFarland turbidity of 0.5.

The new ZOE sealer or control ZOE sealer was

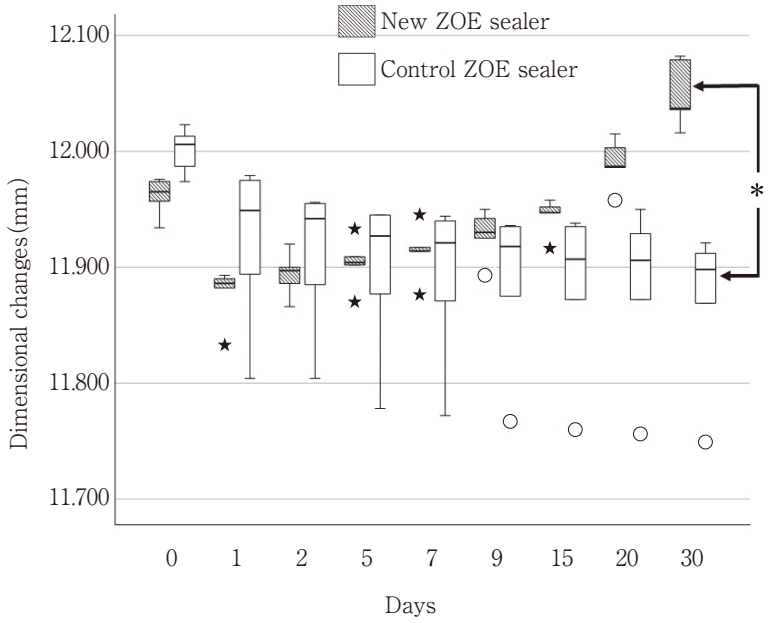

Fig. 1 Size change of sealers

A cylindrical stainless-steel container with a diameter of 6 mm and a height of 12 mm was filled with the new ZOE sealer or control ZOE sealer and stored at 100% relative humidity and 37℃ for 24 h. The container filled with each sealer was immersed in distilled water at 37℃ for 1, 2, 5, 7, 9, 15, 20, and 30 days. The thickness (in millimeters) of the sealer tablet was measured using a micrometer after immersion. This test was repeated five times for each sealer. Outliers are indicated by ○ and extreme outliers by ★. ★ : $p<0.05$, ＊ : $p<0.05$.

applied in a single layer to a filter paper (diameter, 6 mm) after the powder and liquid were mixed. The side of the paper coated with the sealer was placed on an agar medium to culture the *Pi*, *Pg*, or *Ef*.

For *Pi* or *Pg*, the growth inhibition zone from the edge of the filter paper was measured using calipers after 24 h of anaerobic cultivation at 35℃. For *Ef*, the measurement was instead taken after 48 h of aerobic cultivation at 35℃. The area of bacterial growth inhibition was expressed as the length (in millimeters) from the edge of the sealer. This test was repeated twice for each sealer (Table 6).

10. Effects of sealers on performance of composite resins

We investigated the degree of inhibition of polymerization of composite resin materials caused by contact with ZOE sealers.

In this test, two types of composite resins were used: a dual-cure-type composite resin for foundation restoration (UniFil Core EM; GC Corp., Tokyo, Japan) and an adhesive resin cement (ResiCem; SHOFU Inc., Kyoto, Japan). First, the new ZOE sealer or control ZOE sealer was injected into a metal mold and cured by storing at 37℃ and 100% humidity for 24 h. Cured tablets with a diameter of 20 mm and a thickness of 2 mm were produced. A metal frame with an inner diameter of 10 mm and a height of 2 mm was directly placed on these cured sealer tablets, filled with UniFil Core EM or ResiCem, and light-cured for 20 s using a polymerization lamp (XL 3000; 3M, Saint Paul, MN, USA). After storing the photopolymerized specimens at 37℃ and 100% humidity for 24 h, hardness of the composite resin at the interface with each sealer was measured using a Brinell hardness measurement device (MVX-H100; Akashi Seisakusho, Tokyo, Japan)[23]. Hardness (as HB: Brinell hardness number) of the composite resin was obtained as described and compared with that of resins prepared without exposure to the sealers. Hardness of these resins was measured five times for each condition (Table 7).

11. Statistical analysis

For statistical analysis, statistical processing soft-

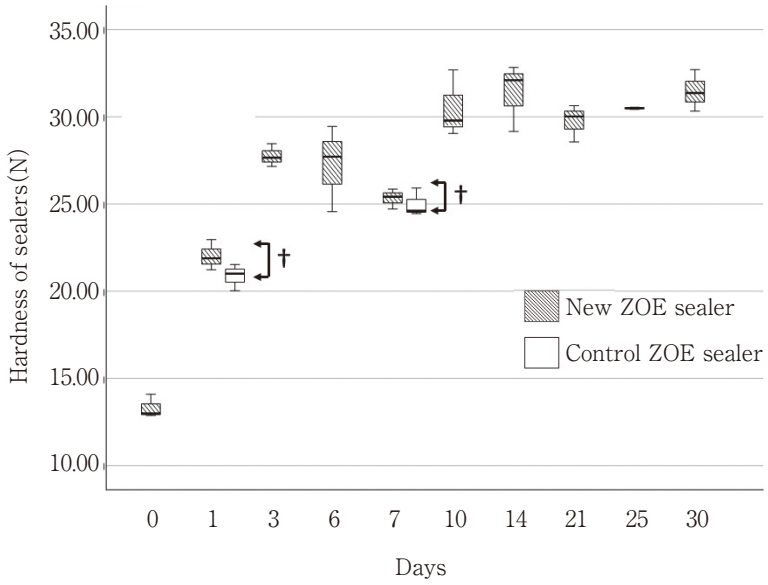

Fig. 2 Hardness of sealers

The new ZOE sealer and control ZOE sealer were cured at 100% relative humidity and 37℃ for 24 h. The cured sealer tablets were immersed in distilled water at 37℃ for 1, 3, 6, 7, 10, 14, 21, 25, and 30 days. In contrast, the cured control ZOE sealer tablets were immersed in distilled water at 37℃ for only 1 and 7 days. The hardness (in Newtons) of these sealer tablets was measured using a texture analyzer. Results are shown as the average of three experimental results. This test was repeated three times for each sealer.
† : $p > 0.05$

Table 6 Preventing bacterial growth with sealers

	Bacterial growth inhibition length (mm)					
	Pi		*Pg*		*Ef*	
	measured value	mean	measured value	mean	measured value	mean
New ZOE sealer	0.990 0.755	0.88	1.010 0.895	0.95	0 0	0
Control ZOE sealer	0.890 1.410	1.15	3.000 1.570	2.29	0 0	0

n=2

The new ZOE sealer or control ZOE sealer was applied in a single layer to a 6-mm-diameter filter paper after the powder and liquid were mixed. The side of the paper coated with sealer was placed on agar medium to culture *Pi*, *Pg*, or *Ef* bacteria.

For *Pi* or *Pg*, the growth inhibition zone from the edge of the filter paper was measured using calipers after 24 h of anaerobic cultivation at 35℃. For *Ef*, this measurement was taken after 48 h of aerobic cultivation at 35℃. The area of bacterial growth inhibition was expressed as the length (in millimeters) from the edge of the sealer. This test was repeated twice for each sealer. This table displays actual measured values obtained from two experiments, along with averaged values.

Table 7 Effects of sealers on composite resin performance

		Brinell hardness
Unifil Core (UC)	UC	61.58±3.12
	UC+New ZOE sealer	60.71±2.88
	UC+Control ZOE sealer	55.16±1.55
		Brinell hardness
ResiCem (RC)	RC	61.61±2.35
	RC+New ZOE sealer	59.84±2.38
	RC+Control ZOE sealer	54.66±2.18

HB; mean±SD, n=5, † : $p>0.05$, ∗ : $p<0.05$

The study investigated the impact of contact with the new ZOE sealer and control ZOE sealer on the polymerization of composite resin materials. Two types of composite resin were utilized: UniFil Core EM (UC), a dual-cure-type composite resin, and ResiCem (RC), an adhesive resin cement.

After storing the photopolymerized resins on cured ZOE sealers at 37℃ and 100% humidity for 24 h, hardness (HB: Brinell hardness number) of the composite resin at the interface with each sealer was measured using a Brinell hardness measurement device. The hardness of the composite resin obtained as described above was compared with that of resins prepared without exposure to sealers. The hardness of these resins was measured five times for each condition.

ware (SPSS Statistics version 28; IBM, Armonk, NY, USA) was used. All experiments except for those shown in Figure 2 and Table 6 were performed five times. The experiment illustrated in Figure 2 was conducted three times, while the experiment shown in Table 6 was performed twice. The significance of differences between the new ZOE sealer group and control ZOE sealer group was calculated with a non-paired means *t*-test for each of Tables 1–5. The experimental results are shown as mean values and standard deviations (SDs). Tests of significance between the two sealers shown in Figure 1 and among the three groups listed in Table 7 were conducted using the Kruskal-Wallis test with Dunn-Bonferroni correction. Values of $p<0.05$ were considered significant.

Results

1. Hardening time of sealers

The hardening time for each sealer was measured at 37℃ and 100% humidity after mixing the powder and liquid. The results are shown in Table 1. Hardening time was significantly shorter for the new ZOE sealer (23.0±1.0 min).

2. Flow behavior of sealers

The viscosity of each sealer was tested immediately after mixing the powder and liquid (Table 2). Viscosity was lower for the new ZOE sealer (22.26±0.47 mm) than for the control ZOE sealer (39.73±1.44 mm). All of these ZOE sealers met the viscosity requirements specified in ISO 6876, being 20 mm or greater.

3. Radiopacity of sealers

Each sealer was stored at 37℃ and 100% humidity for 24 h after mixing the powder and liquid, then radiopacity was measured (Table 3). Radiopacity was lower for the new ZOE sealer (2.6±0.2 mm) than for the control ZOE sealer (3.8±0.5 mm).

4. Solubility of sealers

After each sealer was cured for 24 h at 37℃ and 100% humidity, a disintegration test was conducted (Table 4). The degradation rate did not differ significantly between the new ZOE sealer (0.75±0.19%) and control ZOE sealer (0.55±0.12%; $p=0.088$). The degradation rates of both sealers were below 3%, which is the requirement specified in ISO 6876.

5. Sealing ability of sealers

After filling each sealer into glass tubes, the tubes were immersed in 1% methylene blue solution at 37℃

for 24 h to test marginal sealing ability (Table 5). The new ZOE sealer showed no dye penetration at all (0 mm). In contrast, the marginal sealing ability of the control ZOE sealer was 19.40±0.89 mm.

6. Size change of sealers

The ZOE sealers were placed in cylindrical containers and allowed to cure. After immersing the container filled with sealer in distilled water, the change in volume of the sealer was measured over a 30-day period (Fig. 1). The volume change of ZOE sealer in the container was expressed in terms of sealer thickness.

Thickness of the new ZOE sealer temporarily decreased from the pre-immersion baseline (11.96±0.02 mm) until day 2 after immersion (11.89±0.02 mm), then gradually increased, returning to the original thickness by day 20 (11.99±0.02 mm), and continued to increase after day 30 (12.05±0.03 mm). In contrast, thickness of the control ZOE sealer decreased continuously from the baseline value before immersion (12.00±0.02 mm) to 30 days after immersion (11.87±0.07 mm). After 30 days of immersion in distilled water, the volume of the new ZOE sealer was significantly greater than that of the control ZOE sealer ($p=0.015$).

7. Hardness of sealers

After immersing the cured sealers in distilled water, the change in hardness of the sealers was measured over a 30-day period (Fig. 2). The hardness of the new ZOE sealers before immersion in distilled water was 13.3±0.7 N, increasing to 22.0±0.9 N on day 1 after immersion began. This trend continued until day 3 (27.8 ±0.7 N). After this time, almost no change in hardness was observed. Hardness of the new ZOE sealer on day 7 was 25.3±0.6 N. In contrast, hardness of the control ZOE sealer was 20.9±0.8 N on day 1 and 25.0±0.8 N on day 7. No difference in hardness was observed between the new ZOE sealer and the control ZOE sealer after the same period ($p=1.00$).

8. Preventing bacterial growth with sealers

Each sealer was immediately applied to filter paper after mixing the powder and liquid, and placed on medium cultured with *Pi*, *Pg*, and *Ef*. The distance of the inhibition zone for each bacterium from the edge of the filter paper was then measured (Table 6). Against *Pi*, the new ZOE sealer formed an inhibition zone up to 0.88 mm distance from the edge of the sealer-coated filter paper, while the control ZOE sealer formed an inhibition zone up to 1.15 mm distance. Against *Pg*, the new ZOE sealer formed an inhibition zone up to 0.95 mm distance, whereas the control ZOE sealer formed an inhibition zone up to 2.29 mm distance. Neither the new ZOE sealer nor the control ZOE sealer formed an inhibition circle against *Ef*, indicating no antibacterial activity.

9. Effects of sealers on performance of composite resins

After bonding two types of composite resins (UniFil Core EM and ResiCem) to each cured sealer, the surface hardness of the resins was measured (Table 7).

The surface hardness of UniFil Core EM and ResiCem in contact with the new ZOE sealer did not differ significantly from that of the composite resins cured without sealer ($p=1.00$). In contrast, the surface hardness of UniFil Core EM in contact with the control ZOE sealer was significantly reduced compared to that of the composite resins cured without sealer ($p=0.017$). Additionally, the surface hardness of ResiCem in contact with the control ZOE sealer was significantly reduced compared to that of the composite resins cured without sealer ($p=0.009$).

Discussion

Root canals are treated to achieve a sterile environment and then sealed with antimicrobial materials to prevent bacterial invasion from the oral cavity and periodontal tissues. Materials used for sealing the root canal include gutta-percha and root canal sealers. Root canal sealer is used to fill the space between the inserted gutta-percha point and root canal wall. Until now, the standard sealer has traditionally been a ZOE sealer, as prescribed by Grossman[1].

Recent research has noted that eugenol, which is contained in sealers, can inhibit the adhesion of composite resins to the coronal part of the tooth when present in high concentrations[24,25]. In addition, eugenol can also damage periapical tissues[3,4]. However, eugenol has not only sterilizing effects, but also beneficial pharmacological effects.

Hirafuji et al.[26–28] reported that prostaglandins (PGs) lower the pain threshold in inflamed rat dental pulp. Further, Okiji et al.[29] demonstrated a significant increase in 12-hydroxyeicosatetraenoic acid, a metabolite of arachidonic acid, in rat molar root canals following application of lipopolysaccharide, a bacterial endo-

toxin, compared to the untreated group. Cohen et al.[30] also reported that levels of PGE_2 in the dental pulp of human teeth diagnosed with painful irreversible pulpitis were significantly higher than those in healthy teeth.

On the other hand, we demonstrated that filling a cavity in the rat incisor with ZOE cement significantly suppressed the increase of PGs in the inflamed dental pulp tissue, which was induced by heat and mechanical stimulation, through the release of eugenol from the ZOE[7]. We have also reported that eugenol derived from the ZOE inhibits histamine production[9]. Our previous study revealed that eugenol at concentrations below 10^{-4} M does not induce cell damage or inhibit cell proliferation, collagen formation, or ALP activity in experiments using the osteoblast-like cell line (MC3T3-E1) and rat dental pulp-cultured cells[15]. Hume[2] also speculated that if the concentration of eugenol that penetrates the pulp tissue from ZOE cement is below 10^{-4} M, pharmacological effects such as pain relief and anti-inflammatory effects can be produced in the pulp without risking any tissue damage.

We therefore developed a new ZOE root canal sealer that retains the beneficial antibacterial properties while minimizing irritation to periapical tissues by reducing the eugenol content in the ZOE sealer to approximately 30% of the conventional level.

The hardening process for the new ZOE sealer was completed in 23 min, shorter than that for the control ZOE sealer (1,246 min, Table 1). The setting time for a sealer is related to the root canal filling technique employed by the surgeon. In pressure filling methods that require complex procedures, sealers with longer curing times are preferred. A study into the timing of dental treatment procedures by the Japanese Association for Dental Science[31] reported that the time required for press filling ranged from 14 to 21 min as the number of root canals increased from 1 to 3. The experimental curing time of the new ZOE sealer (23 min) under ISO conditions in this study is considered significantly shorter than the curing time assumed under room temperature and humidity conditions typically found in actual dental practice. Furthermore, the new ZOE sealer is suitable for clinical use because it enables the lateral condensation filling for multiple root canals in around 20 min. Recently, the matched tapered single cone technique has become the most popular method for filling root canals using bioceramic root canal sealers[32]. This method enables the completion of root canal filling in a short time, eliminating the need for extended setting times[33]. The new ZOE sealer is considered suitable for the matched taper single cone technique because of the relatively short setting time. When root canal preparation is performed using the matched taper single cone method, the Ni-Ti rotary file leaves a non-cutting surface. As a result, the condition inside the root canal after the filling procedure greatly depends on the properties of the sealer. We believe that because the eugenol content in the new ZOE sealer is approximately 30% of that in the conventional ZOE sealer, the new sealer is less harmful to tissue and more biocompatible. Also, a longer setting time of sealers is known to increase inflammation in the periapical tissues due to the eugenol released from the sealer[34]. In this regard, the new ZOE sealer sets in a relatively short time and thus appears useful.

The flow behavior test showed that the viscosity of the new ZOE sealer was lower than that of the control ZOE sealer (Table 2). However, the purpose of the flow behavior test is to evaluate the flowability of the sealer within the root canal. All the ZOE sealers in Table 2 met the viscosity requirement specified in ISO 6876, as 20 mm or greater. Flowability of the sealer affects the outcome of root canal filling. With the matched tapered single cone technique, which does not apply pressure during root canal filling, the higher the flowability of the sealer, the easier the adaptation to changes in root canal shape and the better the penetration of dentinal tubules. However, sealers with high fluidity tend to escape outside the apical foramen during root canal filling, so higher biocompatibility is required[35].

X-ray transmittance was equivalent to that seen with aluminum thicknesses of 2.6 mm for the new ZOE sealer and 3.8 mm for the control ZOE sealer (Table 3). With the new ZOE sealer, 20% of the powder material is supplemented with barium sulfate as a contrast agent. In contrast, the control ZOE sealer contains 15% barium sulfate and 15% bismuth subcarbonate to increase radiopacity[20]. The control ZOE sealer is believed to show increased X-ray opacity because it contains 10% more contrast agent than the new ZOE sealer. Radiopacity of the sealer is essential for easily confirming any overflow from the apical foramen on X-ray images after root canal filling. To enhance radiopacity of the new ZOE sealer, it is necessary to con-

sider increasing the amount of contrast material within a range that does not affect the physical properties.

With solubility testing, both the novel ZOE sealer and control ZOE sealer met the ISO 6876 requirement of a degradation ratio less than 3% (Table 4). No significant difference was observed between degradation ratios of the two sealers. Voids created by dissolution of the sealer due to the infiltration of body fluids into the root canal provide habitats for bacteria remaining in the root canal[36]. Root canal filling sealers therefore need to be insoluble over a long period to seal the root canal three-dimensionally.

In the sealing ability test using glass tubes, the new ZOE sealer showed no dye penetration and demonstrated high sealing capability (Table 5). In contrast, the control ZOE sealer exhibited significant pigment penetration (approximately 19 mm). The penetration of dye has already been observed in the root canal sealing experiment using a zinc oxide eugenol sealer with the same composition as the control ZOE sealer used in this experiment, similar to the present results[14]. The dye was considered to have penetrated the gap between the glass tube and the material due to the shrinkage of the sealer. Pulp Canal Sealer, a ZOE-based sealer (Kerr, Brea, CA, USA), has also demonstrated inferior sealing ability compared to AH Plus, an epoxy resin-based sealer (Dentsply Sirona, Ballaigues, Switzerland)[37]. Recently developed bioceramic-based root canal sealers include the bioactive glass-based endodontic sealer[38] and the bioceramic BC sealer[39]. Although neither of these sealers exhibits significant volumetric changes, they have been observed to penetrate deeply into the dentinal tubules. Due to this mechanism, the bioactive glass-based endodontic sealer was thought to result in less dye leakage from the root canal than the conventional ZOE sealer in dye leakage tests using extracted teeth[40]. In this study, we did not conduct penetration tests of the new ZOE sealer itself into the dentinal tubules, nor did we perform dye leakage tests using extracted teeth. However, based on the results of the dye penetration test using a glass tube (Table 5) and the volume change test of the sealer itself (Fig. 1), we believe that the new ZOE sealer has a high ability to seal root canals. On the other hand, while the new ZOE sealer has the potential to cause root fractures due to its expansive properties, we believe that using it together with gutta-percha points, which provide a cushioning effect, significantly reduces the risk of fractures after root canal filling.

In the size change test for the sealers, the new ZOE sealer showed increased volume on day 6 after immersion in distilled water (Fig. 1). The volume of the new ZOE sealer, after being immersed for 30 days, was significantly increased compared to the volume of the control ZOE sealer. This increase in volume of the new ZOE sealer supports the results from the previously mentioned sealing ability test (Table 5), in which the new ZOE sealer blocked dye penetration. Carvalho-Junior et al.[36] reported that the AH Plus sealer expanded by 0.62% after curing in a dimensional change experiment. On the other hand, commonly used ZOE-based sealers are known to shrink during setting[41]. Pressure root canal filling has thus been considered important as a means of correcting for sealer shrinkage. The new ZOE sealer used in this study, however, expanded over time in distilled water, suggesting that expansion may be due to the influence of moisture, such as dentinal tubule fluid within the root canal, during clinical application. In an experiment using a dentin root canal model to observe dimensional changes, methacrylate resin-based sealer was reported to absorb moisture from around the root and to expand during curing[42].

In hardness tests of the sealer, since the new ZOE sealer contains about 30% of the eugenol content of the control ZOE sealer, concerns were raised that not enough chelate bonds might form. This could affect the hardness of the sealer. However, hardness test results for the sealers in this study showed that the new ZOE sealer achieved the same hardness as the control ZOE sealer after immersion in distilled water for both 1 and 7 days (Fig. 2). The new sealer then maintained similar hardness from day 10 through day 30.

After achieving a sterile environment within the root canal, filling of the root canal is performed. However, infected root canals show invasion of microorganisms into the dentinal tubules, and complete removal is reportedly difficult[43,44]. The antibacterial effects of the new ZOE sealer were thus investigated against three types of bacteria commonly found in infected human root canals: *Pi*[45,46], *Pg*[45], and *Ef*[45] (Table 6). The new ZOE sealer formed growth inhibition zones against *Pi* and *Pg*, confirming antibacterial effects for both. In particular, although the amount of eugenol contained in the new ZOE sealer was approximately 30% of that in the

control ZOE sealer, no significant difference was observed in the formation of the inhibition zone for *Pi* growth. Sato et al.[47] pointed out that a longer setting time for the sealer increases the release of eugenol, thereby enhancing antibacterial effects. The antibacterial effect of the sealer may therefore depend on the curing time of the sealer rather than the amount of eugenol it contains.

Eugenol has long been known to be an inhibitor of the curing process in resin-based materials[5,6]. After filling the root canal with sealer, a root canal-retained post core is sometimes directly fabricated using composite resin after a certain period[48]. In this case, curing by light irradiation in the deep areas of the root canal becomes insufficient. Dual-cure composite resins, which utilize both light and chemical curing, are therefore often used. In this experiment, assuming such a situation, the surface hardness of the composite resin core material in contact with the sealer was evaluated (Table 7). The surface hardness of UniFil Core EM and ResiCem in contact with the new ZOE sealer showed no statistically significant difference compared to the surface hardness of these composite resins cured without contact with the new sealer.

However, the surface hardness of both UniFil Core EM and ResiCem in contact with the control ZOE sealer was significantly reduced compared to the surface hardness of the composite resin cured without the control sealer. The amount of eugenol released from the new ZOE sealer thus did not affect the surface hardness of the core material.

Generally, in zinc oxide eugenol sealers, vegetable oil is added to eugenol to improve operability when mixing the powder and liquid[1,20]. In this study, oleic acid was added to the new ZOE sealer to dilute the eugenol, but this did not affect the operability or hardness of the sealer while also improving its sealing ability.

The new ZOE sealer was developed by diluting eugenol with oleic acid to reduce the harmful effects of eugenol released from the sealer on the periapical periodontal tissues after mixing the conventional ZOE sealer. This new sealer expanded slightly after hardening, thus offering not only excellent sealing properties, but also maintenance of antibacterial activity. Further, hardening of the dental composite resin was unaffected.

Conclusions

In this study, we developed a new ZOE sealer by reducing the eugenol content to 30.12% through the use of oleic acid and isostearic acid in the formulation. We then examined the physical properties of the new ZOE sealer, conducted antibacterial tests against three types of bacteria, and clarified the effects of the sealer on the curing of composite resins. The following conclusions were drawn:

1. The curing time of the new ZOE sealer was within 30 minutes. Viscosity and degradation rates met the requirements of ISO 6876.

2. Dye penetration and dimensional change tests revealed that the new ZOE sealer exhibited slight expansion after curing.

3. After curing, the new ZOE sealer displayed comparable hardness to the control ZOE sealer.

4. The new ZOE sealer retained its antibacterial properties against *Pi* and *Pg*, even though it contained only approximately 30% of the eugenol content found in the control ZOE sealer.

5. The new ZOE sealer did not inhibit the curing of two types of composite resin used in core construction.

These excellent properties of the new ZOE sealer suggest potential utility for clinical application as a root canal filling sealer.

Conflict of interest

There are no conflicts of interest to disclose regarding this paper.

References

1) Grossman LI. An improved root canal cement. J Am Dent Assoc 1958; 56: 381–385.
2) Hume WR. The pharmacologic and toxicologic properties of zinc oxide-eugenol. J Am Dent Assoc 1986; 113: 789–791.
3) Briseño BM, Willershausen B. Root canal sealer cytotoxicity on human gingival fibroblasts. I, Zinc oxide-eugenol-based sealers. J Endodo 1990; 16: 383–386.
4) Gulati N, Chandra S, Aggarwal PK, Singh M. Cytotoxicity of eugenol in sealer containing zinc-oxide. Dent Traumatol 1991; 7: 181–185.
5) Bayindir F, Akyil MS, Bayindir YZ. Effect of eugenol and non-eugenol containing temporary cement on perma-

nent cement retention and microhardness of cured composite resin. Dent Mater J 22, 592–599, 2003.
6) Wongsorachai RN, Thanatvarakorn O, Prasansuttiporn T, Jittidecharaks S, Hosaka K, Foxton RM, Nakajima M. Effect of polymerization accelerator on bond strength to eugenol-contaminated dentin. J Adhes Dent 2018; 20: 541–547.
7) Hashimoto S, Uchiyama K, Maeda M, Ishitsuka K, Furumoto K, Nakamura Y. *In vivo* and *in vitro* effects of zinc oxide-eugenol (ZOE) on biosynthesis of cyclo-oxygenase products in rat dental pulp. J Dent Res 1988; 67: 1092–1096.
8) Hashimoto S, Maeda M, Yamakita J, Nakamura Y. Effects of zinc oxide-eugenol on leucocyte number and lipoxygenase products in artificially inflamed rat dental pulp. Arch Oral Biol 1990; 35: 87–93.
9) Maeda M, Hashimoto S, Ishitsuka K, Nakamura Y. Filling effect of zinc oxide-eugenol (ZOE) on histamine levels in inflamed pulps of rat mandibular incisors. Jpn J Conserv Dent 1994; 37: 1864–1877.(in Japanese)
10) Markowitz K, Moynihan M, Liu M, Kim S. Biologic properties of eugenol and zinc oxide-eugenol. A clinically oriented review. Oral Surg Oral Med Oral Pathol 1992; 73: 729–737.
11) Gerosa R, Borin M, Menegazzi G. *In vitro* evaluation of the cytotoxicity of pure eugenol. J Endod 1996; 22: 532–534.
12) Hashieh IA, Camps J, Dejou J, Franquin JC. Eugenol diffusion through dentin related to dentin hydraulic conductance. Dent Mater 1998; 14: 229–236.
13) Chang YC, Tai KW, Huang FM, Huang MF. Cytotoxic and nongenotoxic effects of phenolic compounds in human pulp cell cultures. J Endod 2000; 26: 440–443.
14) Okiji T, Watanabe I, Izawa T, Araki K, Suda H, Sunada I. A study on the new root canal sealer (NU-59), Part Ⅰ: Evaluation of sealing ability. Jpn J Conserv Dent 1986; 29: 1710–1716.(in Japanese)
15) Ishitsuka K, Hashimoto S, Toen T, Katsuumi I. Effects of eugenol on the shape and function of cultured cells from rat dental pulps. Jpn J Conserv Dent 2000; 43: 1063–1073.(in Japanese)
16) Hume WR. An analysis of the release and diffusion through dentin of eugenol from zinc oxide-eugenol mixtures. J Dent Res 1984; 63: 881–884.
17) Hume WR. *In vitro* studies on the local pharmacodynamics, pharmacology and toxicology of eugenol and zinc oxide-eugenol. Int Endod J 1988; 21: 130–134.
18) Mikami M. Cell-biological study on the significance of pulp capping materials to human pulp fibroblast. Kanagawa Shigaku 1992; 26: 353–371.(in Japanese)
19) Inventor: Hashimoto S, Maeda M, Ishitsuka K, Katsuumi I, Applicant: Bee Brand Medico Dental Co Ltd, Title of Invention: Dental composition. The patent application was submitted to the Japan Patent Office as a worldwide patent on October 30, 2008 (JP2008279157A). The patent was published on May 13, 2010 (JP2010105953A) and was granted on September 4, 2013 (P5280801).
20) Shima S, Mitomo K, Hatogai H, Takahashi H, Nakagawa K, Okada T, Ito A, Asai Y. Experimental studies on the setting properties of various kinds of root canal sealers and pastes in vitro, with special reference to zinc oxide eugenol preparations. Shikagakuho 1980; 80: 211–223.(in Japanese)
21) ISO standards 6876. Dental root canal sealing materials. Geneva, Switzerland : International Organization for Standardization ; 2001.
22) Ogura Y, Katsuumi I. Setting properties and sealing ability of hydraulic temporary sealing materials. Dent Mater J 2008; 27: 730–735.
23) Suzuki J, Okada S, Yokota K, Tsunekawa M, Teranaka T, Tani-Ishii N. Effect of zinc oxide-eugenol root canal sealers on resin materials—Brinell hardness of resin surfaces in contact with ZOE sealers and pull-out bond strength in root canals—. Jpn J Conserv Dent 2011; 54: 297–305.(in Japanese)
24) Boone KJ, Murchison DF, Schindler WG, Walker WAⅢ. Post retention: the effects of sequence of post-space preparation, cementation time, and different sealers. J Endod 2001; 27: 768–771.
25) Hagge MS, Wong RD, Lindemuth JS. Retention strengths of five luting cements on prefabricated dowels after root canal obturation with a zinc oxide/eugenol sealer: 1. Dowel space preparation/cementation at one week after obturation. J Prosthodont 2002; 11: 168–175.
26) Hirafuji M, Satoh S, Ogura Y. Prostaglandins in rat pulp tissue. J Dent Res 1980; 59: 1535–1540.
27) Hirafuji M, Terashima K, Satoh S, Ogura Y. Stimulation of Prostaglandins E_2 biosynthesis in rat dental pulp explants *in vitro* by 5-hydroxytryptamine. Archs Oral Biol 1982; 27: 961–964.
28) Hirafuji M. Inhibition of prostaglandin I_2 biosynthesis in rat dental pulp by phenolic dental medicaments. Jpn J Pharmacol 1984; 36: 544–546.
29) Okiji T, Morita I, Kobayashi C, Sunada I, Murota S. Arachidonic-acid metabolism in normal and experimentally-inflamed rat dental pulp. Archs Oral Biol 1987; 32: 723–727.
30) Cohen JS, Reader A, Fertel R, Beck FM, Meyers WJ. A radioimmunoassay determination of the concentration of prostaglandins E_2 and $F_{2\alpha}$ in painful and asymptomatic human dental pulps. J Endod 1985; 11: 330–335.
31) Time study of dental treatment procedures 2016 edition. Japanese Association for Dental Science. https://www.

jads.jp/assets/pdf/time_study/time_study_y2016.pdf (cited 2025.7.18)
32) Guivarc'h M, Jeanneau C, Giraud T, Pommel L, About I, Azim AA, Bukiet F. An international survey on the use of calcium silicate-based sealers in non-surgical endodontic treatment. Clin Oral Investig 2020; 24: 417–424.
33) Morotomi T. Basic knowledge of current root canal sealers and root canal filling methods. Jpn J Conserv Dent 2024; 67: 245–250.(in Japanese)
34) Loushine BA, Bryan TE, Looney SW, Gillen BM, Loushine RJ, Weller RN, Pashley DH, Tay FR. Setting properties and cytotoxicity evaluation of a premixed bioceramic root canal sealer. J Endod 2011; 37: 673–677.
35) Kwak SW, Koo J, Song M, Jang H, Gambarini G, Kim H-C. Physicochemical properties and biocompatibility of various bioceramic root canal sealers: *in vitro* study. J Endod 2023; 49: 871–879.
36) Carvalho-Junior JR, Correr-Sobrinho L, Correr AB, Sinhoreti MAC, Consani S, Sousa-Neto MD. Solubility and dimensional change after setting of root canal sealers: a proposal for smaller dimensions of test samples. J Endod 2007; 33: 1110–1116.
37) Vo K, Daniel J, Ahn C, Primus C, Komabayashi T. Coronal and apical leakage among five endodontic sealers. J Oral Sci 2022; 64: 94–98.
38) Washio A, Nakagawa A, Nishihara T, Maeda H, Kitamura C. Physicochemical properties of newly developed bioactive glass cement and its effects on various cells. J Biomed Mater Res 2015; 103: 373–380.
39) Komabayashi T, Colmenar D, Cvach N, Bhat A, Primus C, Imai Y. Comprehensive review of current endodonteic sealers. Dent Mater J 2020; 39: 703–720.
40) Washio A, Morotomi T, Yoshii S, Kitamura C. Bioactive glass-based endodontic sealer as a promising root canal filling material without semisolid core materials. Materials (Basel) 2019; 29; 12: 3967.
41) Ørstavik D, Nordahl I, Tibballs JE. Dimensional change following setting of root canal sealer materials. Dent Mater 2001; 17: 512–519.
42) Furuta K, Saigusa K, Murayama F, Sekiya M, Nishida T, Maeda M, Igarashi M. Effect of the wet environment around the root on dimensional changes in resin-based root canal sealers during setting in human extracted teeth. ODEP 2024; 4: 36–45.
43) Noiri Y, Ehara A, Kawahara T, Takemura N, Ebisu S. Participation of bacterial biofilms in refractory and chronic periapical periodontitis. J Endod 2002; 28: 679–683.
44) Matsuo T, Shirakami T, Ozaki K, Nakanishi T, Yumoto H, Ebisu S. An immunohistochemical study of the localization of bacteria invading root pulpal walls of teeth with periapical lesions. J Endod 2003; 29: 194–200.
45) Pinto KP, Barbosa AFA, Silva EJN, Santos APP, Sassone LM. What is the microbial profile in persistent endodontic infections? A scoping review. J Endod 2023; 49: 786–798.
46) Heyder M, Kranz S, Völpel A, Pfiser W, Watts DC, Jandt KD, Sigusch BW. Antibacterial effect of different root canal sealers on three bacterial species. Dent Mater 2013; 29: 542–539.
47) Sato T, Suzuki J, Yokota K, Tsunekawa M, Hamada N, Tani-Ishii N. The physical properties and antimicrobial effect of newly- developed paste-type root canal sealers. JJEA 2009; 30: 125–131.(in Japanese)
48) Farid F, Mahgoli H, Hosseini A, Chiniforush N. Effect of eugenol-containing and resin endodontic sealers on retention of prefabricated metal posts cemented with zinc phosphate and resin cements. J Prosthodont Res 2013; 57: 284–287.

Original Article

ODEP 6 (1) : 14～22, 2026

Usefulness of Aspartate Aminotransferase Measurement in Gingival Crevicular Fluid as an Indicator of Periodontal Disease Progression

Hiroshi ITO, Yukihiro NUMABE, Satoshi SEKINO, Shunsuke TAKEYA, Norihiro TSUNODA* and Miyako KODAMA*

Department of Periodontology, The Nippon Dental University School of Life Dentistry at Tokyo
*The Nippon Dental University Hospital at Tokyo, General Dentistry

Abstract

Purpose: The creation of a chairside system for predicting periodontal disease progression is a requirement for next-generation periodontal examination. Aspartate aminotransferase (AST), which is observed in gingival crevicular fluid (GCF), could be a marker for assessing tissue damage in clinical practice. The purpose of this study was to examine whether measurement of AST in GCF is effective as an indicator of periodontal disease progression during the supportive periodontal therapy (SPT) phase.

Methods: GCF samples were randomly collected from 122 sites on single-rooted teeth in the upper and lower jaws of 40 patients who had transitioned to the SPT stage. GCF samples were collected at the time of SPT transition (baseline), and AST levels in the GCF were measured using an AST measurement kit along with periodontal examinations. Periodontal examination items at the GCF collection sites included plaque index, probing depth (PD), clinical attachment level (CAL), gingival index, and bleeding on probing (BOP). The study protocol included a 3-month recall and a 12-month observation period. Logistic regression analysis was performed using sites with PD ≥4 mm and BOP (+) at 12 months as the pathological condition, with this condition as the dependent variable.

Results: On logistic regression analysis, for the objective variable, a positive result of the AST measurement kit showed a significantly higher odds ratio compared to a negative result, and a CAL ≥5 mm at the time of transition to SPT also showed a significantly higher odds ratio compared to a CAL <5 mm.

Conclusion: A positive result from the AST measurement kit indicates the possibility of the continuation and progression of periodontitis. In other words, the information obtained from the use of the AST measurement kit can be an indicator that strongly supports active periodontal treatment intervention during the SPT phase to stabilize the condition of periodontal disease.

Key words: gingival crevicular fluid, aspartate aminotransferase, periodontal examination

Corresponding author: Hiroshi ITO, Department of Periodontology, The Nippon Dental University School of Life Dentistry at Tokyo, 1-9-20, Fujimi, Chiyoda-ku, Tokyo 102-8159, Japan
TEL: +81-3-3261-2473, FAX: +81-3-3264-5937, E-mail: hiroshi@tky.ndu.ac.jp
Received for Publication: December 17, 2025/Accepted for Publication: February 18, 2026
DOI: 10.11471/odep.2026-002

Introduction

Periodontitis, which is strongly associated with decline of oral function including tooth loss, is a chronic disease with a high incidence rate[1]. Although periodontitis does not cause obvious pain in the early stages, by the time patients become aware of the symptoms, they often find that loss of attachment has led to decreased oral function[2]. Given this background, one of the goals of modern periodontal treatment is to detect the early periodontal disease stage and perform minimally invasive periodontal treatment to prevent the progression of periodontal disease, restore oral function, and prevent recurrence of periodontal disease. To achieve these purposes, it is important to plan treatment based on the results of examinations such as probing depth (PD), clinical attachment level (CAL), and bleeding on probing (BOP), which are obtained through precise probing techniques to determine the pathological condition of periodontal disease. However, the probing procedure requires delicate techniques that can be painful and burdensome for the patient[3], and the positive predictive value of BOP test results has been reported to be low[4]. Therefore, as a prerequisite for next-generation periodontal examination, it is necessary to establish a system that can detect the progression of periodontal disease at the chairside and easily determine the precise state of the disease. To achieve this, it is necessary to identify potential tissue damage markers that reflect the state of the disease, and it is hoped that this approach will be applied to daily clinical practice.

Currently, gingival crevicular fluid (GCF) is attracting attention for analyzing periodontal tissue markers in periodontal disease as samples can be collected non-invasively and reflect tissue damage at the sampling site[2,5,6]. Our group has reported that there is a high possibility of discrepancies between the results of the BOP test[4], which is the foundation of periodontal examination as the results can effectively predict the possibility of attachment loss, and clinical symptoms[7]. Therefore, we proposed that one of the factors contributing to the discrepancy is the limitation of the BOP test, which is determined by visual inspection, and hypothesized that invisible bleeding occurs even when the BOP test result is negative (BOP (−)). We have previously reported that hemoglobin (Hb), which is evidence of a history or the presence of bleeding, can be observed using an immunochromatography (IC) method even in BOP (−) cases, and that it may be a potential marker of tissue damage and a useful indicator that can strongly complement BOP testing[8,9]. Furthermore, a longitudinal observational study also found that aspartate aminotransferase (AST), measured using enzyme activity analysis, behaves similarly to Hb and may be a potential marker of tissue damage[10]. AST is an enzyme present within cells, but it escapes from the cells due to tissue damage and is observed in GCF. It has been reported to show a high correlation with periodontal examination results, and is expected to be a potential marker of tissue damage[11–16].

Currently, clinical applications of AST measurement kits that enable semi-quantitative evaluation of AST levels have been reported to be useful for determining the prognosis of periodontal treatment and evaluating dynamic periodontal treatments, and as an indicator for determining the recall interval during supportive periodontal therapy (SPT)[17–22]. However, no reports have examined the possibility that AST measurement kits could help identify the progression of periodontal disease during the SPT phase. Therefore, using the current AST measurement kit, the Periodontal Tissue Monitor (PTM) kit (Shofu Inc., Kyoto, Japan), new possibilities for measuring AST levels in GCF were investigated by examining whether the kit can be used as a tool to predict the progression of periodontal disease.

Materials and Methods

1. Experimental design

This was a longitudinal, observational study designed according to the STROBE guidelines and conducted in accordance with the 1975 Declaration of Helsinki, as revised in 2013. All patients participating in the study were given a full explanation of the purpose and intent of the study, and informed consent was obtained. They also signed up in writing before participating in the study.

2. Study population

The study participants were patients with chronic periodontitis who had entered the SPT stage and whose condition was judged to be generally stable as a result of a re-evaluation examination after periodontal

treatment while visiting the Nippon Dental University Hospital. The inclusion criteria were in accordance with our previous studies[7-10]. Study participants were non-smokers with at least 12 remaining teeth[23] and in good general health. The exclusion criteria were:(1) patients with endocrine and metabolic diseases, malignant tumors, immune diseases, liver diseases, renal failure, heart diseases, or osteoporosis;(2) pregnant women or patients taking contraceptives; and (3) patients who did not consent to participate in this study. At the time of transition to SPT, there was a mixture of patients who had undergone periodontal surgery and those who had not, and this study included both groups.

3. Research protocol

The monitoring and sampling periods for this first-time study were from September 2022 to May 2024. The monitoring period was one year, and the recall interval was three months(0, 3, 6, 9, and 12 months). At each recall, a special periodontist (HI) recorded clinical parameters, provided oral hygiene instructions, and performed professional tooth cleaning[24]. If necessary, subgingival debridement was performed using an ultrasonic device by HI. The transition to SPT was at baseline (BL), which was set at 0 months, the start of this study. At BL, in addition to each periodontal examination, a PTM kit test assessment was also performed (Fig. 1).

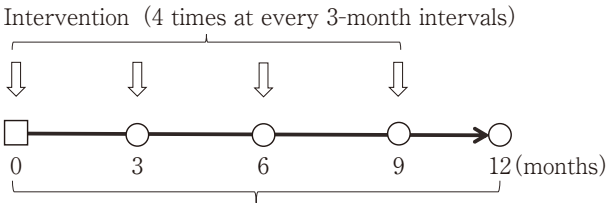

○: Periodontal examinations+Treatment intervention; 3, 6, 9, 12 months
□: Periodontal examinations+Treatment intervention+PTM kit test; 0 months

Fig. 1 Research protocol

The recall interval was 3 months, and periodontal examinations included PlI, PD, CAL, GI, and BOP. SPT included oral hygiene instruction, professional teeth cleaning, and subgingival debridement as needed. The time of SPT transition was BL. The PTM kit was used only at the time of BL (0 months).

BL: baseline, PlI: plaque index, PD: probing depth, CAL: clinical attachment level, GI: gingival index, BOP: bleeding on probing, SPT: supportive periodontal therapy

4. Measurements of clinical parameters

Periodontal examinations for all patients were performed by a HI certified by the Japanese Society of Periodontology, who was blinded to all patient information. The clinical parameters were measured by HI in the following order: plaque index (PlI)[25], PD, CAL, gingival index (GI)[26], and BOP. The pocket probe used for each clinical parameter was the WILLIAMS PROBE (Hu-Friedy Inc., IL, USA). The BOP test was performed according to the methods of Ainamo et al.[27] and Armitage et al.[28]. The calibration to HI achieved 100% agreement (n=10) between the first and second recordings at 24-hour intervals for PD and CAL measurements.

5. GCF collection

The sampling site was determined according to the criteria of previous studies[7-10]. Pockets for the target teeth were randomly selected from single-rooted anterior teeth (central incisors, lateral incisors, canines, and premolars) in the maxilla and mandible. The exclusion criteria for GCF sampling sites were abutment teeth for fixed bridges, anchor teeth for removable partial dentures, and implants.

6. AST detection using the PTM kit

The PTM kit test and analysis were performed strictly according to the protocol and evaluated using a known AST level (1,200 μIU) to measure the presence of inflammation. Regarding the setting of a known AST level, previous studies have reported that an AST level of 1,200 μIU is useful for classifying healthy and inflamed sites in periodontal tissues, and that it may correlate with each clinical parameter. It has also been reported to be useful for periodontal treatment intervention. Therefore, an AST level of 1,200 μIU was determined to be reasonable[18,19,21,29]. GCF sampling was performed at a room temperature of 23℃ using dedicated absorbent filter paper (Shofu Inc.). To prevent blood contamination by the probing, GCF was collected after PlI measurement. The clinical parameters PD, CAL, GI, and BOP were then recorded. For the GCF sampling method, supra-gingival plaque was removed as much as possible, and a sterile roll cotton filter was placed on the pocket opening area for 30 seconds while drying with a mild air syringe. The filter paper with sampled GCF was reacted for exactly 6 minutes according to the PTM kit protocol, and the color intensity compared with the standard solution was judged

Table 1 Classification of periodontitis in patients (n=40) (Tonetti et al., 2018)

Stage	I			II			III			IV		
Grade	A	B	C	A	B	C	A	B	C	A	B	C
Localized chronic periodontitis	7	−	−	8	−	−	−	−	−	−	−	−
Generalized chronic periodontitis	−	−	−	−	−	−	2	2	−	1	16	4

and recorded. The PTM kit test results were assessed in a separate examination space by another dentist (ST), not HI, who was not aware of patient information. If bleeding occurred due to insertion of the filter paper, the GCF sample was considered to be contaminated with blood and was excluded. Also, if the sample was excluded, the reaction time was exceeded.

7. Statistical analysis

Statistical analysis was performed by a special periodontist (SS) who was blinded to patient information and the periodontal examination results, including the PTM kit test results. The statistical software used for analysis was SPSS ver. 22.0 J (IBM-SPSS, Inc., NY, USA). Statistical analysis was performed using the Kolmogorov-Smirnov test followed by Spearman's correlation coefficient. In the BOP test results, BOP (−) was represented as 0 and BOP (+) as 1, and for the PTM kit test results,"no inflammation" (−) was represented as 0 and "inflammation" (+) was represented as 1 for analysis. For the analysis, 0 months was defined as BL, and the results of the periodontal examination 12 months later were compared using the Wilcoxon signed-rank test. In addition, the results of periodontal tests 12 months later were examined for areas that showed positive results in the PTM kit analysis. The comparison was between areas that did and did not show attachment loss using the Mann-Whitney *U*-test. Furthermore, areas with PD≥4 mm accompanied by BOP (+) at the time of periodontal examination 12 months later were defined as unhealthy conditions[30,31], and a logistic regression analysis was performed using this as the dependent variable. The explanatory variables were a positive PTM kit test result at BL, CAL ≥5 mm at BL, and plaque adhesion at BL. On statistical analysis, $p<0.05$ was taken to indicate a significant difference.

Results

1. Patients

The 40 participants consisted of 14 men and 26 women (70.5±17.4 years old), and GCF was collected from 122 sites. The classification of periodontitis in patients[32] is shown in Table 1. Furthermore, no dropouts due to various reasons were observed in this study. The breakdown of the 122 sites from which GCF was collected for the 40 participants was as follows: 1 site in 5, 2 sites in 10, 3 sites in 7, 4 sites in 15, 5 sites in 2, and 6 sites in 1. Table 2 shows the tooth types from which GCF was collected. The Kolmogorov-Smirnov test showed that the clinical parameters were not normally distributed. The confounding factors and stratified analysis of the participants were examined as follows.

A significance test was performed using Fisher's exact test with a 2×2 contingency table for the area of increased CAL after PTM test results. Comparisons were performed by classifying patients into stage I/II and stage III/IV. No significant differences were found in the two groups. Therefore, the trends were similar, and no obvious confounding factors were identified.

2. Comparison of clinical parameters at BL and 12 months later

Comparing the periodontal examination results at BL and at the 12-month recall, significant decreases were observed in GI and BOP, whereas the slight increases in PlI, PD, and CAL were not significant (Table 3).

3. Correlations between PTM kit test results and each clinical parameter at BL

Significant correlations were observed between PTM kit test results and each clinical parameter (Table 4).

4. Changes in clinical parameters when a PTM kit test result was positive

For the sites that showed a positive PTM kit test

Table 2 Classification of inspection sites

	Upper	Lower
Central incisor	20	7
Lateral incisor	13	15
Canine	19	28
Premolar	1	19

The tooth types at the 122 sites from which gingival crevicular fluid was collected.

Table 3 Changes in periodontal examinations between BL and 12 months (122 sites)

		PlI	PD	CAL	GI	BOP
BL	Mean	0.93	3.53	4.62	1.52	0.62
	SD	0.75	1.60	2.30	0.71	0.49
p-value		0.538	0.886	0.062	<0.001	0.008
12 months	Mean	0.98	3.54	4.68	1.28	0.48
	SD	0.76	1.69	2.36	0.74	0.50

Comparisons between clinical parameters at BL and the final recall were analyzed using the Wilcoxon signed-rank test. P-values were rounded to four decimal places. For statistical analysis, negative (−) and positive (+) results of the BOP test were quantified as 0 and 1, respectively. BL: baseline, PlI: plaque index, PD: probing depth, CAL: clinical attachment level, GI: gingival index, BOP: bleeding on probing, SD: standard deviation

Table 4 Correlations with clinical parameters and PTM kit test results (n=122 sites)

PlI	CC	0.338
	SP	<0.001**
PD	CC	0.440
	SP	<0.001**
CAL	CC	0.442
	SP	<0.001**
GI	CC	0.731
	SP	<0.001**
BOP	CC	0.791
	SP	<0.001**

Correlation coefficient (CC)
Significant probability (SP)
**: p<0.01

Significant correlations were seen between the PTM kit test results and all clinical parameters. PlI: plaque index, PD: probing depth, CAL: clinical attachment level, GI: gingival index, BOP: bleeding on probing

result, a comparison was made at BL between 7 areas where CAL increased and 60 areas where CAL remained unchanged or decreased in each clinical parameter 12 months later. From the results, the PD in areas where CAL increased was a significantly deeper pocket than in areas where CAL remained unchanged or decreased. Furthermore, the results of this study showed that, in cases with a positive PTM kit test result, the rate of disease progression, which showed an increase in CAL, was 10.4%. The 95% confidence interval (CI) for the area of increased CAL was calculated as 5.2–20.0% using the Wilson scoring method (Table 5).

5. Logistic regression analysis

Multivariate logistic regression analysis using the PD status of PD ≥4 mm with BOP(+)at the time of recall 12 months later as the dependent variable indicated that a positive PTM kit test result showed a significantly higher odds ratio compared with a negative PTM kit test result (adjusted odds ratio=3.38), and CAL ≥5 mm at BL also showed a significantly higher odds ratio compared with CAL <5 mm (adjusted odds ratio=4.43). However, no significant correlation was observed for PlI (adjusted odds ratio=0.56) (Table 6).

Discussion

One of the goals of the GCF component analysis was to extract markers that can contribute to pre-symptomatic diagnosis as indicators of attachment loss. From a report on the analysis of biochemical components of GCF, biochemical components of GCF that show a high correlation with clinical parameters such as PD and BOP are thought to be markers that can strongly complement the diagnostic testing of periodontal disease, and their selection has been actively pursued[2,5,6]. However, analyses using existing clinical parameters, particularly the BOP test, have reported that the frequency of test results is a predictor of the occurrence of attachment loss[4]. In recent years, attempts have been made to identify markers observed in GCF that are involved in the pre-symptomatic diagnosis of periodontal disease. In particular, the identification of markers that are specifically expressed in clini-

Table 5 Changes in clinical parameters when a PTM kit test result was positive

		PlI	PD	CAL	GI	BOP
Measurement values at BL in sites where CAL increased after 12 months	Mean	1.14	6.00	6.14	2.00	1.00
	SD	0.38	2.24	2.12	0.00	0.00
p-value		0.555	0.008	0.320	0.554	0.554
Measurement values at BL in sites where CAL was unchanged or decreased after 12 months	Mean	1.17	3.87	5.43	1.95	0.97
	SD	0.69	1.76	2.58	0.29	0.18

If a PTM kit test result was positive, the CAL increased at 12 months at those sites, and sites with CAL unchanged or decreased from BL were compared using the Mann-Whitney *U*-test. P-values were rounded to four decimal places. BL: baseline, PlI: plaque index, PD: probing depth, CAL: clinical attachment level, GI: gingival index, BOP: bleeding on probing

Table 6 Objective variable: Areas with PD≧4 mm and BOP-positive at follow-up by multivariate logistic regression analysis

	Adjusted odds ratio	95%CI	p value
PTM kit test result (+)	3.38	1,19–9,60	0.022
CAL≧5 mm at BL	4.43	1,72–11,44	0.002
PlI at BL	0.56	0,19–1,68	0.303

A positive PTM kit test result was associated with a significantly higher odds ratio than a negative PTM kit test result (adjusted odds ratio=3.38), and a CAL≧5 mm at BL was associated with a significantly higher odds ratio than a CAL<5 mm (adjusted odds ratio=4.43). However, no significant association was observed for PlI (adjusted odds ratio=0.56). BL: baseline, PD: probing depth, CAL: clinical attachment level, BOP: bleeding on probing, PlI: plaque index, CI: confidence interval

cally stable conditions, such as those showing BOP(−), has attracted attention[7–9].

Previous studies of the progression of periodontal disease have suggested that matrix metalloproteinases in GCF[33,34] and subgingival bacteria such as *Porphyromonas gingivalis* and *Treponema denticola* are potential markers that should be measured[35]. In addition, some reports have suggested that the ratio of *P. gingivalis* to total bacteria in saliva samples and the *P. gingivalis* IgG antibody titer in serum may be associated with the progression of periodontitis[36,37]. Recently, AST has attracted attention as one of the GCF components that reflects the progression stage of periodontal disease, and reports on its clinical application have been accumulating[17–22]. Previous reports using animal models have already shown a correlation between the progression of inflammation and AST levels[11], and clinical studies have shown a correlation with clinical parameters in periodontal disease examinations[12–14]. Furthermore, from the decrease of AST levels from periodontal treatment, its clinical usefulness as an indicator for determining prognosis after periodontal treatment is recognized[20,22].

In this study, the relationships between PTM kit test results and periodontal examinations were investigated, and, as in previous studies, high correlations with periodontal disease test results were demonstrated. These results demonstrate that measuring AST in GCF effectively improves the accuracy of periodontal examinations, which was one of the goals of this study, and lays the groundwork for a new method of using the PTM kit that can contribute to stabilizing the condition of periodontal disease.

Considering that the study period was one year (12 months), periodontal disease progression was defined as a periodontal examination after 12 months showing pockets ≧4 mm and a positive BOP test[30,31]. In this case, logistic regression analysis showed that the progression of periodontal disease was associated with the presence of CAL ≧5 mm at BL, as well as a positive PTM kit test result. The importance of pocket management was reiterated[38,39]. Furthermore, when the PTM kit test result at BL was positive, attachment loss was observed in approximately 10% of cases at the periodontal examination 12 months later. In other words, the results of the assessment using the PTM kit test can contribute to determining whether the periodontal disease condition will continue during the SPT stage, and can be a powerful indicator that can strongly support active periodontal treatment intervention to stabi-

lize the condition.

The results of the present study suggest that longer-term observation is necessary to use "no loss of attachment" as an indicator of disease stability[31]. Furthermore, taking into account the possibility of systemic disease occurring as the subjects age, consideration should also be given to each life stage, incorporating oral health-related quality of life (QOL)[40]. During this observation period, attachment loss was observed in some sites in patients with a positive PTM kit test result. Furthermore, the outcome of this study is considered to be an event showing attachment loss of 2 mm or more with BOP (+). We also plan to use an event in which a BOP (−) site shifts to BOP (+) as a surrogate endpoint. In the future, we plan to conduct follow-up surveys and closely monitor the patients who participated in this study. In addition, we believe that longitudinal multi-center studies that take into consideration 1) each life stage, 2) types of systemic disease, and 3) application to multi-rooted teeth, are required.

Conclusion

From this study, a positive PTM kit test result indicates the possibility of continuation and progression of periodontitis. In other words, a positive PTM kit test result may be an indicator that can strongly support active periodontal treatment intervention during the SPT phase to achieve stabilization of periodontal disease.

Funding information

This study was supported by Grants-in-Aid from the Ministry of Education and Science Research Funds (Grant Nos. C, JP20K09964, JP20K09981, JP23K09189) and a grant from the "New medical equipment and technology industry vision" project of the Japan Dental Association.

Compliance with ethical standards

This study was conducted in accordance with the Helsinki Declaration of 1975, as revised in 2013, with approval from the ethics committee of the Nippon Dental University (Approval No. NDU-T 2021-11).

Conflict of interest

The authors received the PTM kit from Shofu Inc., Kyoto, Japan, but the company had no role in the study design, data collection, analysis, or manuscript preparation.

Author contributions

Hiroshi Ito: Formal analysis; Measurement of clinical parameters; GCF collection; Methodological verification; Investigation; Validation; Writing-review & editing; Writing-original draft. Yukihiro Numabe: Funding acquisition; Patient selection; Methodological verification; Investigation; Validation; Writing-review & editing; Writing-original draft. Satoshi Sekino: Investigation; Methodology; Validation; Statistical analysis. Shunsuke Takeya: Investigation; Methodology; Validation, GCF analysis. Norihiro Tsunoda: Patient selection; Writing-review & editing; Writing-original draft. Miyako Kodama: Patient selection; Writing-review & editing; Writing-original draft.

References

1) Page RC, Kornman KS. The pathogenesis of human periodontitis: an introduction. Periodontol 2000 1997; 14: 9–11.
2) Buduneli N, Biyikoğlu B, Kinane DF. Utility of gingival crevicular fluid components for periodontal diagnosis. Periodontology 2000 2024; 95: 156–175.
3) Heft MW, Perelmuter SH, Cooper BY, Magnusson I, Clark WB. Relationship between gingival inflammation and painfulness of periodontal probing. J Clin Periodontol 1991; 18: 213–215.
4) Lang NP, Joss A, Orsanic T, Gusberti FA, Siegrist BE. Bleeding on probing. A predictor for progression of periodontal disease? J Clin Periodontol 1986; 13: 590–596.
5) Loss BG, Tjoa S. Host-derived diagnostic markers for periodontitis: do they exist in gingival crevice fluid? Periodontol 2000 2005; 39: 53–72.
6) Gupta S, Chhina S, Arosa SA. A systematic review of biomarkers of gingival crevicular fluid: Their predictive role in diagnosis of periodontal status. J Oral Biol Craniofac Res 2018; 8: 98–104.
7) Ito H, Numabe Y, Sekino S, Murakashi E, Iguchi H, Hashimoto S, Sasaki D, Yaegashi T, Kunimatsu K, Takai H, Mezawa M, Ogata Y, Watanabe H, Hagiwara S, Izumi Y, Hiroshima Y, Kido JI, Nagata T. Evaluation of bleeding on probing and gingival crevicular fluid enzyme activity for detection of periodontally active sites during supportive periodontal therapy. Odontology 2014; 102: 50–56.
8) Ito H, Numabe Y, Sekino S, Murakashi E, Ishiguro H, Hashimoto S, Sasaki D, Yaegashi T, Takai H, Mezawa M, Ogata Y, Watanabe H, Hagiwara S, Izumi Y, Hiroshima Y, Kido JI, Nagata T, Kunimatsu K. Correlation between gingival crevicular fluid hemoglobin content and periodontal clinical parameters. J Periodontol 2016;

87: 1314–1319.
9) Ito H, Numabe Y, Hashimoto S, Uehara S, Wu YH, Ogawa T. Usefulness of hemoglobin examination in gingival crevicular fluid during supportive periodontal therapy to diagnose the pre-symptomatic state in periodontal disease. Clin Oral Invest 2021; 25: 487–495.
10) Ito H, Numabe Y, Sekino S, Murakashi E, Ishiguro H, Hashimoto S, Sasaki D, Yaegashi T, Takai H, Mezawa M, Ogata Y, Watanabe H, Izumi Y, Hiroshima Y, Kido JI, Nagata T. Utility of a haemoglobin test of gingival crevicular fluid: A multicentre, observational study. Oral Dis 2024; 30: 1533–1542.
11) Cohen RL, Alves MEAF, Crawford JM, McSwiggin T, Chambers DA. Association of gingival crevicular fluid aspartate aminotransferase levels with histopathology during ligature-induced periodontitis in the beagle dog. J Dent Res 1991; 70: 984–987.
12) Nakamura T, Kido JI, Kido R, Ohishi K, Yamauchi N, Kataoka M, Nagata T. The association of calprotectin level in gingival crevicular fluid with gingival index and the activities of collagenase and aspartate aminotransferase in adult periodontitis patients. J Periodontol 2000; 71: 361–367.
13) Persson RG, DeRouen TA, Page RC. Relationship between gingival crevicular fluid levels of aspartate aminotransferase and active tissue destruction in treated chronic periodontitis patients. J Periodont Res 1990; 25: 81–87.
14) Persson RG, Page RC. Diagnostic characteristics of crevicular fluid aspartate aminotransferase (AST) levels associated with periodontal disease activity. J Clin Periodontol 1992; 19: 43–48.
15) Chambers DA, Imrey PB, Cohen RL, Crawford JM, Alves ME, McSwiggin TA. A longitudinal study of aspartate aminotransferase in human gingival crevicular fluid. J Periodont Res 1991; 26: 65–74.
16) Magnusson I, Persson RG, Page RC, DeRouen TA, Crawford JM, Cohen RL, Chambers DA, Alves ME, Clark WB. A multi-center clinical trial of a new chairside test in distinguishing between diseased and healthy periodontal sites. II. Association between site type and test outcome before and after therapy. J Periodontol 1996; 67: 589–596.
17) Persson RG, Alves MEAF, Chambers DA, Clark WB, Cohen R, Crawford JM, DeRouen TA, Magnusson I, Schindler T, Page RC. A multicenter clinical trial of PerioGard™ in distinguishing between diseased and healthy sites (I). Study design, methodology and therapeutic outcome. J Clin Periodontol 1995; 22: 794–803.
18) Shimada K, Mizuno T, Uchida T, Kato T, Ito K, Murai S. Relationship between levels of aspartate aminotransferase in gingival crevicular fluid and conventional measures of periodontal status assessed using PocketWatch™: A cross-sectional study. J Oral Sci 1999; 41: 35–40.
19) Shimada K, Mizuno T, Ohshio K, Kamaga M, Murai S, Ito K. Analysis of aspartate aminotransferase in gingival crevicular fluid assessed by using PocketWatch™: a longitudinal study with initial therapy. J Clin Periodontol 2000; 27: 819–823.
20) Kamma JJ, Nakou M, Persson RG. Association of early onset periodontitis microbiota with aspartate aminotransferase activity in gingival crevicular fluid. J Clin Periodontol 2001; 28: 1096–1105.
21) Takei M, Nakayama Y, Toyoshima I, Hiromatsu Y, Ikeda Y, Ogata Y. Comparison of the levels of aspartate aminotransferase and clinical parameters pre- and post-initial therapy and periodontal surgery. J Jpn Soc Periodontol 2015; 56: 390–398. (in Japanese)
22) Nakayama Y, Takei-Obi M, Toyoshima-Matsumura I, Tsutamori M, Kato A, Okano C, Mezawa M, Ogata Y. Clinical usability of aspartate aminotransferase to evaluate the prognosis of periodontal regeneration therapies: prospective, longitudinal study. Odontology 2018; 106: 306–315.
23) Reissmann DR, Wolfart S, John MT, Marré B, Walter M, Kern M. Kohal R, Nothdurft F, Stark H, Schierz O, Wöstmann B, Hannak W, Mundt T, Pospiech P, Boldt J, Edelhoff D, Busche E, Jahn F, Luthardt RG, Hartmann S, Heydecke G. Impact of shortened dental arch on oral health-related quality of life over a period of 10 years—A randomized controlled trial. J Dent 2019; 80: 55–62.
24) Herbert FW, Thomas MH. Color atlas of dental hygiene: Periodontology. Thieme: Stuttgart; 2006. 242–243.
25) Löe H. The gingival index, the plaque index and the retention index systems. J Periodontol 1967; 38: 610–616.
26) Silness J, Löe H. Periodontal disease in pregnancy II. Correlation between oral hygiene and periodontal condition. Acta Odontol Scand 1964; 22: 112–135.
27) Ainamo J, Bay I. Problems and proposals for recording gingivitis and plaque. Int Dent J 1975; 25: 229–235.
28) Armitage GC, Svanberg GK, Löe H. Microscopic evaluation of clinical measurements of connective tissue attachment levels. J Clin Periodontol 1997; 4: 173–190.
29) Richard JO, Howard H, Marc LN, David SR, Gordon HD, Julio S, Joseph PF. Relationship between crevicular aspartate aminotransferase levels and periodontal disease progression. J Periodontol 2001; 72: 17–24.
30) Claffey N, Nylund K, Kiger R, Garrett S, Egerberg J. Diagnostic predictability of score plaque, bleeding, suppuration and probing depth for attachment loss. 3 1/2 years of observation following initial periodontal therapy. J Clin Periodontol 1990; 17: 108–114.

31) Matuliene G, Pjetursson BE, Salvi GE, Schmidlin K, Brägger U, Zwahlen M, Lang NP. Influence of residual pockets on progression and tooth loss: results after 11 years of maintenance. J Clin Periodontol 2008; 35: 685–695.
32) Tonetti MS, Greenwell H, Korman KS. Staging and grading of periodontitis: framework and proposal of a new classification and case definition. J Clin Periodontol 2018; 45 (Suppl 20): S149–61.
33) Kinney JS, Morelli T, Braun T, Ramseier CA, Herr AE, Sugai JV, Shelburne CE, Rayburn LA, Singh AK, Giannobile WV. Saliva/pathogen biomarker signatures and periodontal disease progression. J Dent Res 2011; 90: 752–758.
34) Kinney JS, Morelli T, Oh M, Braun TM, Ramseier CA, Sugai JV, Giannobile WV. Crevicular fluid biomarkers and periodontal disease progression. J Clin Periodontol 2014; 41: 113–120.
35) Byrne SJ, Dashper SG, Darby IB, Adams GG, Hoffmann B, Reynolds EC. Progression of chronic periodontitis can be predicted by the levels of Porphyromonas gingivalis and Treponema denticola in subgingival plaque. Oral Microbiol Immunol 2009; 24: 469–477.
36) Sugi N, Naruishi K, Kudo C, Hisaeda-Kako A, Kono T, Maeda H, Takashiba S. Prognosis of periodontitis recurrence after intensive periodontal treatment using examination of serum IgG antibody titer against periodontal bacteria. J Clin Lab Anal 2011; 25: 25–32.
37) Nomura Y, Shimada Y, Hanada N, Numabe Y, Kamoi K, Sato T, Gomi K, Arai T, Inagaki K, Fukuda M, Noguchi T, Yoshie H. Salivary biomarkers for predicting the progression of chronic periodontitis. Arch Oral Biol 2012; 57: 413–420.
38) Lang NP, Matulień G, Salvi GE, Tonetti MS. Supportive periodontal therapy. Lang NP, Lindhe J. Clinical periodontology and implant dentistry. 6th ed. Wiley: West Sussex; 2015. 1347–1371.
39) Merin RL. Supportive periodontal treatment. Newman MG, Takei HH, Klokkevold PR, Carranza FA. Clinical Periodontology. 13th ed. Elsevier: Philadelphia; 2019. 714–723.
40) FDI World Dental Federation. FDI policy statement on oral health and quality of life Adopted by the FDI General Assembly. Int Dent J 2016; 66: 11–12.

Original Article

ODEP 6 (1) : 23〜29, 2026

Effect of Enamel Surface Topography on Demineralization

Takako EGUCHI, Ryouichi SATOU[1], Ryo SAKO[2], Masahiro FURUSAWA[2] and Naoki SUGIHARA[1]

Department of Dental Hygiene, Tokyo Dental Junior College
[1]Department of Epidemiology and Public Health, Tokyo Dental College
[2]Department of Endodontics, Tokyo Dental College

Abstract

Purpose: Enamel, which covers the tooth crown surface, is highly susceptible to acidic components found in food and beverages. In recent years, dental erosion resulting from demineralization by dietary acids has received increasing attention. Habitual intake of acidic foods and beverages is recognized as a major contributor to the increasing prevalence of acid erosion. Previous studies have reported that the extent of enamel demineralization varies depending on the type of organic acid present in food, such as phosphoric acid, citric acid, acetic acid, and lactic acid. However, the influence of enamel surface properties, particularly variations in smoothness or roughness, on susceptibility to demineralization remains insufficiently understood. Therefore, this study aimed to determine the extent to which enamel surfaces with different surface properties are affected under acidic conditions, and to evaluate the effectiveness of smoothing treatments—specifically tooth surface polishing—in suppressing demineralization.

Methods: Twenty-eight bovine mandibular incisors were used to prepare the specimens. After demineralization with a citric acid solution, surface roughness and Vickers hardness (Hv) were measured for each experimental group.

Results: The results demonstrated an increase in surface roughness (Sa) across all groups following immersion in the acidic solution. This change was particularly pronounced in the rough group, where roughness increased progressively with longer immersion times. Furthermore, a significant decrease in Hv was observed in all groups, with the rough group exhibiting the largest ΔHv values.

Conclusion: These findings indicate that maintaining a smooth enamel surface helps suppress demineralization and suggest that tooth surface polishing procedures designed to enhance surface smoothness may play an important role in preventing acid erosion.

Key words: enamel, surface roughness, hardness, tooth surface polishing

Corresponding author: Ryouichi SATOU, Department of Epidemiology and Public Health, Tokyo Dental College, 2-9-18, Kanda-Misakicho, Chiyoda-ku, Tokyo 101-0061, Japan
TEL: +81-3-6380-9272, FAX: +81-3-6380-9606, E-mail: satouryouichi@tdc.ac.jp
Received for Publication: December 24, 2025/Accepted for Publication: May 20, 2026
DOI: 10.11471/odep.2026-003

Introduction

Enamel, which covers the crown surface of the tooth, is highly susceptible to acidic components present in food and beverages. In recent years, increasing attention has been directed toward dental erosion, a condition characterized by enamel demineralization caused by dietary acids. Dental erosion is defined as the chemical dissolution of tooth structure in the absence of bacterial involvement[1]. The etiological factors contributing to acid erosion can be broadly categorized into endogenous and exogenous. Endogenous factors include chronic gastrointestinal conditions, such as gastroesophageal reflux disease. Exogenous factors include the consumption of acidic foods and beverages commonly ingested in daily life, including citrus fruits, carbonated beverages, sports drinks, and alcoholic beverages[2]. Furthermore, acid erosion has been reported among workers in battery manufacturing plants and related industries where strong acids such as hydrochloric acid and sulfuric acid are routinely handled, indicating that occupational acid exposure also represents an important contributing factor[3].

Among these factors, habitual consumption of acidic foods and beverages is regarded as the primary driver of the recent increase in acid erosion. Previous studies have reported that the type of organic acid present, such as phosphoric, citric, acetic, or lactic acid, can influence the extent of enamel demineralization[4]. However, the impact of variations in enamel surface properties, particularly surface roughness, on susceptibility to demineralization remains unclear. Therefore, this study aimed to clarify the extent to which enamel surfaces with different surface characteristics are affected under acidic conditions, and to evaluate the effectiveness of smoothing treatments, specifically tooth surface polishing, in suppressing enamel demineralization.

Materials and Methods

1. Preparation of enamel specimens

A total of 28 bovine mandibular incisors were used in this study. The cervical and incisal regions were sectioned using a diamond band saw (KT100, Maruto Co., Ltd., Tokyo, Japan) under continuous water cooling, and the central crown enamel was excised. The labial enamel surface of each crown was then polished to a mirror finish using waterproof abrasive paper (#120–1200; Sankei Co., Ltd., Tokyo, Japan) followed by Metaserve (Spectrographic Ltd., London, UK), until the polished surface was parallel to the measuring table[5].

2. Demineralization experiments

A citric acid solution (0.1 mol, pH 4.0) was prepared, based on the acids and concentrations typically found in soft drinks, for use in the demineralization experiments[4]. Considering the polishing condition and citric acid immersion time, the prepared samples were assigned to the experimental groups presented in Table 1. Each sample was immersed in 5 mL of the citric acid solution.

3. Observation method

1) Three-dimensional measurement by laser scanning microscope

Surface roughness was evaluated using a three-dimensional laser scanning microscope (LEXT OLS4000, Olympus Co., Tokyo, Japan). Surface roughness was measured at five locations on each sample using arithmetic mean roughness (Sa), and the mean and standard deviation were calculated. The measurement area was set to 645×645 μm, with a cutoff value of 80 μm[6,7]. Comparisons were conducted between groups before and after the demineralization experiments, and the change in Sa was calculated as ΔSa=before demineralization experiment−after demineralization experiment.

2) Observation using a microhardness tester

Hardness measurements were performed using a microhardness tester (HMV-1, Shimadzu Co., Kyoto, Japan). An indentation load of 1.961 N was applied for 20 seconds for each measurement. Vickers hardness (Hv) was calculated from the diagonal length of the indentation using the standard formula[7,8]. Measurements were taken at five locations on each sample, and the mean and standard deviation were determined. Comparisons were made between the groups before and after the demineralization experiments, and the change in Hv values before and after demineralization was calculated as ΔHv=pre-demineralization experiment−post-demineralization experiment.

4. Statistical analysis

All experimental data were analyzed using the statistical software Origin2022 (2022, Lightstone Corp, Tokyo, Japan). Differences between the groups were assessed using one-way analysis of variance. Following the iden-

Table 1 Overview of the experimental groups

Experimental group		Polishing condition	Immersion time
Coarse group	A	#120 only	2 minutes
	B	#120 only	6 minutes
Smooth group	C	#120–1200	2 minutes
	D	#120–1200	6 minutes

The samples were randomly divided into four groups (n=7 per group) based on the surface polishing condition and immersion time.

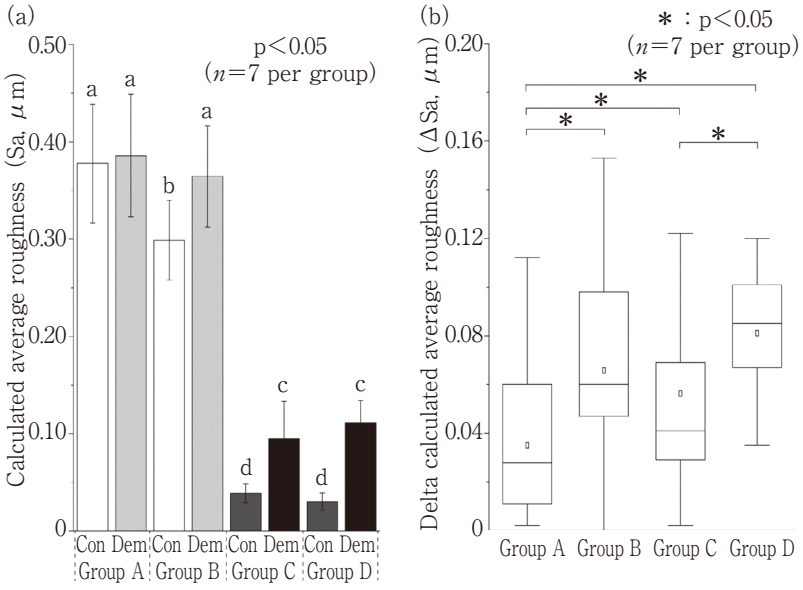

Fig. 1 Surface roughness measurements

(a) Results are expressed as mean values and standard deviations. Identical lowercase letters indicate no significant difference between values ($p<0.05$). Con: Control (reference surface), Dem: Demineralization (experimental surface)

(b) Difference (ΔSa) in surface roughness (Sa) values between the reference surface and experimental surface.

tification of significant differences, Tukey-Kramer's post-hoc test was performed for multiple comparisons. A p-value of <0.05 was considered significant.

Results

1. Surface roughness measurement

The results of the Sa measurements are presented in Fig. 1. In Group A, the Sa value before the demineralization experiment was $0.378\pm0.061\,\mu$m, increasing slightly to $0.386\pm0.063\,\mu$m after the experiment. The corresponding pre- and post-experiment values were $0.299\pm0.041\,\mu$m and $0.364\pm0.051\,\mu$m in Group B, $0.039\pm0.010\,\mu$m and $0.095\pm0.038\,\mu$m in Group C, and $0.030\pm0.009\,\mu$m and $0.111\pm0.023\,\mu$m in Group D, respectively. An increase in the Sa value was observed in all groups after the demineralization experiment (Fig. 1-a). Analysis of the ΔSa values revealed significant differences between Groups A and B, Groups A and C, Groups A and D, and Groups C and D (Fig. 1-b).

2. Hardness measurement

The results of Hv measurements are presented in Fig. 2. A decrease in Hv value was observed in all groups after the demineralization experiment (Fig. 2-a),

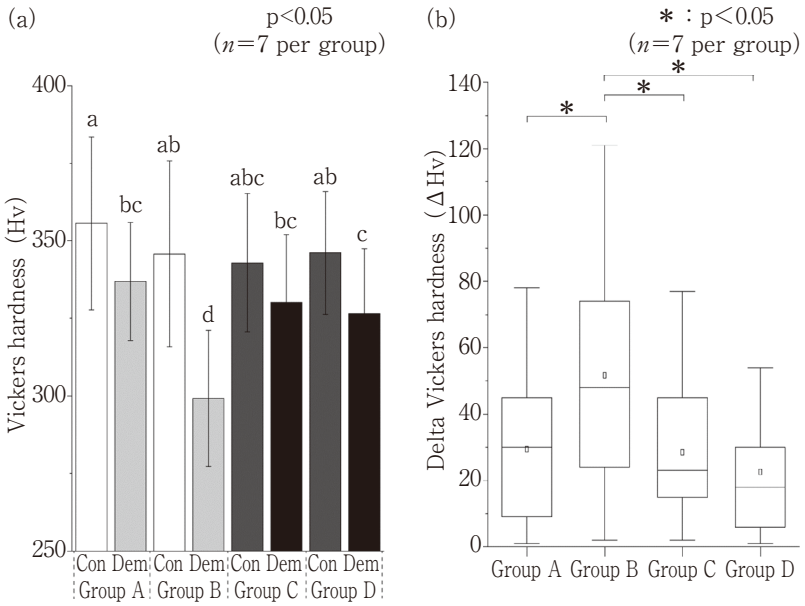

Fig. 2 Vickers hardness measurements

(a) Results are expressed as mean values and standard deviations. Identical lowercase letters indicate no significant difference between values ($p<0.05$). Con: Control (reference surface), Dem: Demineralization (experimental surface)

(b) Difference (ΔHv) in Vickers hardness (Hv) values between the control surface and experimental surface.

with Group B exhibiting the greatest reduction. Analysis of ΔHv values revealed significant differences between Groups A and B, Groups B and C, and Groups B and D (Fig. 2-b).

Discussion

Numerous studies have investigated enamel demineralization caused by dietary acids, with many focusing on the effects of acid type, pH, and immersion duration[9-11]. However, the influence of enamel surface structure on susceptibility to dietary acids remains unclear. Accordingly, to elucidate this relationship the present study examined the effects of dietary acids, particularly citric acid, on enamel surface structure.

1. Comparison of surface roughness

Comparisons of Sa levels before and after the demineralization experiments across groups showed an increasing trend in all groups, though no significant differences were observed between some groups. Furthermore, ΔSa values were analyzed among the groups. In the rough groups (Groups A and B), ΔSa was 0.008 μm in Group A and 0.065 μm in Group B, indicating an approximately eight-fold greater increase in Group B than in Group A. The smooth-surface groups (Groups C and D) also exhibited an increasing trend in ΔSa, with statistically significant differences observed. As the differences between Groups A and B and between Groups C and D were attributable to immersion time in citric acid solution rather than to the polishing condition, these variations were presumed to result from the time-dependent progression of demineralization. Kono et al. reported that when human enamel was immersed in carbonated beverages, Hunter-Schreger bands were observable after 1 day; however, after 7 days of immersion, the enamel surface normalized, and the Hunter-Schreger bands were nearly absent[12]. Furthermore, Zero et al. suggested that citric acid, commonly present in soft drinks, may act as a chelating agent, promoting demineralization by binding to and leaching calcium from enamel and dentin[3]. Accordingly, the marked increase in ΔSa values observed in the rough group in the present study is likely attributable to the combined effects of time-dependent demineralization and the calcium-chelating action of citric acid.

2. Comparison of hardness measurement results

Regarding Hv measurements, reductions in Hv values were observed in all groups before and after the demineralization experiment, with significant differences confirmed between the groups. As the primary difference in experimental conditions among groups was immersion time, these results suggest that demineralization progresses over time, consistent with the surface roughness findings. Analysis of ΔHv values revealed a significant difference between the rough groups (Groups A and B), whereas no significant difference was found between the smooth groups (Groups C and D). This pattern was thought to be due to the greater reduction in hardness caused by demineralization in the rough groups (Groups A and B) compared with the relatively smaller reduction in the smooth groups (Groups C and D). Sugito et al. reported that tooth staining is influenced by natural pigments in spices and by the surface roughness of the tooth surface[13]. In the present study, coarsely polished (rough group) and finely polished groups (smooth group) were created by varying the polishing state of the enamel surface. The coarsely polished group exhibited a significant decrease in hardness. Similar to the mechanism proposed for tooth staining, the increased surface roughness of the coarsely polished enamel likely enlarged the effective surface area, increasing the contact with the acid solution. This greater exposure rendered the surface more susceptible to acid attack, leading to more pronounced demineralization.

3. Tooth surface polishing

Dental caries and periodontal disease are highly prevalent oral conditions that can significantly affect quality of life[14]. Effective prevention of these diseases requires inhibiting the formation and adhesion of dental plaque, the primary causative agent, and plaque control is recognized as a key strategy to achieve this[15]. As chemical removal of plaque is extremely challenging, mechanical methods are currently recognized as the most effective approach[16]. One widely used mechanical method is professional mechanical tooth cleaning (PMTC), a system proposed by Axelsson et al.[17], Klock[18], Needleman et al.[19] in which dentists or dental hygienists employ specialized rotary instruments and polishing paste to thoroughly remove dental deposits and plaque.

The cleaning efficacy of pastes used in PMTC depends on the characteristics of the abrasive particles, with the type and particle shape influencing their ability to clean and polish the tooth surface[20]. These properties are quantitatively evaluated using the radioactive dentin abrasivity (RDA) and pellicle cleaning ratio (PCR) values[21]. Although the relationship between RDA and PCR values and polishing effectiveness remains a subject of some debate, these parameters serve as useful indicators for selecting a PMTC paste tailored to each patient's individual oral environment.

In general, the cleaning performance and polishing ability of PMTC pastes depend on the material composition, and these two properties are often in conflict[22,23]. Consequently, PMTC pastes with different RDA values are commonly applied in a multi-step, sequential procedure. In recent years, one-step PMTC pastes capable of performing both cleaning and finishing with a single product have been developed, and studies have reported their effectiveness[24]. Nevertheless, the selection of products and the method of applying them remain at the discretion of the practitioner. The final condition of the tooth surface likely depends on multiple factors, including the materials used, the practitioner's skill, and the initial state of the enamel. Therefore, future studies should investigate these factors in conjunction with the results of this study.

In this study, experimental conditions were established using a combination of polishing brushes, cups, and polishing pastes, and the effects were compared under roughened and smoothed tooth surface conditions. In future research, more detailed experimental parameters, such as paste particle size, brush design, and applied polishing pressure, should be considered to further clarify their respective effects on tooth surface characteristics.

Conclusion

This study investigated the effects of food-derived acids, particularly citric acid, on enamel demineralization using Sa and Hv as indicators, with a focus on variations in surface polishing and immersion time. Following demineralization, Sa values increased in all groups. However, the rough group exhibited a significantly larger change, approximately eight times greater than that observed in the smooth group, as immersion time increased. Furthermore, Hv decreased significantly in

all groups, with the rough group showing the greatest ΔHv values. These findings suggest that a rougher enamel surface increases the contact area with acid, making it more susceptible to acid-induced demineralization. Surface roughness, in particular, emerged as a significant factor affecting the reduction in tooth hardness. Maintaining a smooth enamel surface appears to be effective in suppressing demineralization. Tooth surface polishing, which enhances enamel smoothness, plays a critical role in preventing tooth demineralization. Further studies are warranted because this study evaluated only two enamel surface conditions, namely smooth and rough surfaces. Future investigations should examine the effects of acid exposure on tooth surfaces with intermediate characteristics while also considering the presence of the pellicle.

Conflict of Interest

The authors declare no conflicts of interest related to this paper.

Acknowledgments

The authors would like to thank Tokyo Dental College for granting access to the Oral Science Research Center and all individuals who contributed to this study.

References

1) Marqués Martínez L, Leyda Menéndez AM, Ribelles Llop M, Segarra Ortells C, Aiuto R, Garcovich D. Dental erosion. Etiologic factors in a sample of valencian children and adolescents. Cross-sectional study. Eur J Paediatr Dent 2019; 2: 189–193.
2) Zero DT. Etiology of dental erosion—extrinsic factors. Eur J Oral Sci 1996; 104: 162–177.
3) Zero DT, Lussi A. Erosion—chemical and biological factors of importance to the dental practitioner. Int Dent J 2005; 55: 285–290.
4) Eguchi T, Satou R, Miake S, Sugihara N. Comparison of resistance of dentin to erosive acid after application of fluoride to teeth. J Hard Tissue Biology 2020; 26: 193–202.
5) Miake Y, Nozue S, Moriguchi M, Yamazaki T, Sawada T, Yanagisawa T. The ability of xylitol containing gum with calcified seaweed in preventing demineralization of tooth surfaces. J Hard Tissue Biol 2011; 20: 87–92.
6) Noro A, Kaneko M, Murata I, Yoshinari M. Influence of surface topography and surface physicochemistry on wettability of zirconia (tetragonal zirconia polycrystal). J Biomed Mater Res B Appl Biomater 2013; 101B: 355–363.
7) Satou R, Miki N, Iwasaki M, Sugihara N. Fully automated bioreactor-based pH-cycling system for demineralization: a comparative study with a conventional method. Materials (Basel) 2023; 16: 4929.
8) Miki N, Miake Y, Shimoda S, Mishima H. Evaluation of enamel acid resistance and whitening effect of the CAP system. Dent J (Basel) 2022; 10: 161.
9) Harper RA, Shelton RM, James JD, Salvati E, Besnard C, Korsunsky AM, Landini G. Acid-induced demineralization of human enamel as a function of time and pH observed using X-ray and polarized light imaging. Acta Biomater 2021; 120: 240–248.
10) Kolumban A, Moldovan M, Tig IA, Chifor I, Cuc S, Bud M, Badea ME. An evaluation of the demineralizing effects of various acidic solutions. Appl Sci 2021; 11: 8270.
11) Mylonasa P, Austina RS, Moazzezb R, Joinerc A, Bartletta DW. In vitro evaluation of the early erosive lesion in polished and natural human enamel. Dent Mater 2018; 34: 1391–1400.
12) Kono T, Watanabe A, Kanno T, Ootani Y, Tamamura R, Sakae T, Okada H. Carbonated soft drink-soaking changes the crystallographic properties of human tooth enamel—a micro-XRD study. J Hard Tissue Biology 2019; 28: 129–138.
13) Sugito H, Eguchi T, Tanaka R, Haruyama A, Muramatsu T. The effects of dietary pH changes on tooth staining of the enamel surface. ODEP 2023; 3: 80–85.
14) Axelsson P, Nyström B, Lindhe L. The long-term effect of a plaque control program on tooth mortality, caries and periodontal disease in adults. J Clin Periodontol 2004; 31: 749–757.
15) Nomura Y, Takeuchi H, Kaneko N, Matin K, Iguchi R, Toyoshima Y, Kono Y, Ikemi T, Imai S, Nishizawa T, Fukushima K, Hanada N. Feasibility of eradication of mutans streptococci from oral cavities. J Oral Sci 2004; 46: 179–183.
16) Axelsson P, Londhe J, Wäseby J. The effect of various plaque control measures on gingivitis and caries in schoolchildren. Community Dent Oral Epidemiol 1976; 4: 232–234.
17) Axelsson P, Lindhe J. Effect of controlled oral hygiene procedures on caries and periodontal disease in adults. J Clin Periodontol 1978; 5: 133–151.
18) Klock B. Long-term effect of intensive caries prophylaxis. Community Dent Oral Epidemiol 1984; 12: 69–71.
19) Needleman I, Nibali L, Di Iorio A. Professional mechanical plaque removal for prevention of periodontal disease in adults—systematic review update. J Clin Periodontol 2015; 42: 12–35.

20) Barnes CM. The science of polishing. Dimens Dent Hyg 2009; 7: 18–22.
21) Li Y. Stain removal and whitening by baking soda dentifrice: a review literature. J Am Dent Assoc 2017; 148: 20–26.
22) Barbakow F, Imfeld T, Luz F, Stookey G, Schemehorn B. Dentin abrasion (RDA), enamel abrasion (REA) and polishing scores of dentifrices sold in Switzerland. Schweiz Monatsschr Zahnmed 1989; 99: 408–413.
23) Schemeborn BR, Moore MH, Putt MS. Abrasion, polishing, and stain removal characteristics of various commercial dentifrices in vitro. J Clin Dent 2011; 22: 11–18.
24) Amari Y, Takamizawa T, Kawamoto R, Namura Y, Murayama R, Yokoyama M, Tsujimoto A, Miyazaki M. Influence of one-step professional mechanical tooth cleaning pastes on surface roughness and morphological features of tooth substrates and restoratives. J Oral Sci 2021; 63: 133–138.

Original Article

ODEP 6 (1) : 30～37, 2026

Cdc42 Inhibition Compromises the Junctional Epithelial Barrier via Decreased Adhesion Molecule Levels and the Induction of Pro-inflammatory Responses

Daisuke SAITO, Ryo AIZAWA, Masaru SUNAGA and Matsuo YAMAMOTO

Division of Periodontology, Department of Conservative Dentistry, Showa Medical University School of Dentistry

Abstract

Purpose: The junctional epithelium (JE) serves as the primary line of host defense at the dentogingival interface. The role of Cdc42 in regulating the barrier function of the JE remains largely unknown. This study aimed to investigate the role of the small GTPase Cdc42 in regulating JE barrier function, inflammatory responses, and adhesion molecule expression using the murine JE cell line JE-1 and the selective Cdc42 inhibitor ML141.

Methods: JE-1 cells were treated with ML141, and cell viability was assessed using a 3-(4,5-dimethylthiazol-2-yl)-2,5-diphenyltetrazolium bromide assay to determine the non-cytotoxic concentration. Epithelial barrier function was evaluated via a fluorescein isothiocyanate (FITC)-dextran permeability assay. Additionally, quantitative real-time polymerase chain reaction was performed to analyze the gene expression levels of inflammatory mediators (*Il1b*, *Il6*, *Mmp12*) and various cell adhesion molecules (*Cldn1*, *Gja1*, *Itgb4*, *Dst*, *Col17a1*, *Dsp*, *Dsg3*).

Results: Treatment with 10 μM ML141 did not significantly affect JE-1 cell viability, but resulted in a significant increase in epithelial permeability. Cdc42 inhibition led to significant upregulation of the pro-inflammatory genes *Il1b*, *Il6*, and *Mmp12*. Furthermore, the expression levels of key intercellular and hemidesmosomal adhesion molecules (*Cldn1*, *Gja1*, *Itgb4*, *Dst*, *Col17a1*, *Dsp*, *Dsg3*) were markedly decreased following ML141 treatment.

Conclusion: These findings demonstrate that Cdc42 plays a critical role in maintaining the structural integrity and homeostasis of the JE. Pharmacological inhibition of Cdc42 compromises epithelial barrier function, induces a pro-inflammatory phenotype, and significantly reduces the expression of adhesion molecules. Consequently, Cdc42 dysfunction may contribute to the breakdown of the periodontal epithelial barrier.

Key words: junctional epithelium, Cdc42, barrier function

Corresponding author: Ryo AIZAWA, Division of Periodontology, Department of Conservative Dentistry, Showa Medical University School of Dentistry, 2-1-1, Kitasenzoku, Ohta-ku, Tokyo 145-8515, Japan

TEL: +81-3-3787-1151, FAX: +81-3-3787-9290, E-mail: r-aizawa@dent.showa-u.ac.jp

Received for Publication: April 14, 2026/Accepted for Publication: May 20, 2026

DOI:10.11471/odep.2026-004

Introduction

Periodontitis is a chronic inflammatory disease characterized by the progressive destruction of tooth-supporting tissues, including the resorption of alveolar bone and the loss of connective tissue attachment[1]. It is widely recognized as a multifactorial condition driven by complex interactions between microbial pathogens, environmental risk factors, and the host immune response[2]. The invasion of periodontopathic bacteria through the gingival sulcus, where the epithelial barrier functions as the primary line of host defense, is key to the onset of this disease[3].

At the forefront of this defensive barrier lies the junctional epithelium (JE), situated at the base of the gingival sulcus[3]. The JE is structurally distinct from the oral gingival and sulcular epithelia. It is a non-keratinized squamous epithelium with a high turnover rate[4]. Morphologically, the JE is attached directly to the tooth surface (enamel or cementum) via hemidesmosomes[5]. Unlike other epithelia that rely heavily on tight and adherens junctions for sealing, the JE exhibits sparse intercellular junctions and poorly developed desmosomes, resulting in an intrinsically permeable barrier[6].

Small GTPases belonging to the Rho family are molecular switches that regulate a wide variety of signaling pathways in all eukaryotic cells. RhoA, Rac1, and Cdc42 are the best-characterized members of the small Rho GTPases, and among them, Cdc42 plays a crucial role in regulating the actin cytoskeleton, cell polarity, microtubule dynamics, membrane transport pathways, and transcription factor activity[7]. It has been suggested that RhoA plays a role in the attachment of the JE to the tooth surface[8]. In typical epithelial models, such as the intestinal epithelium and keratinocytes, Cdc42 has been shown to be essential for maintaining barrier function and regulating intercellular junctions, including tight junctions[9]. While we have previously established a murine JE cell line (JE-1) that recapitulates key biological features of the tissue[10], little is known about the role of Cdc42 in intercellular adhesion or epithelial barrier function in the JE.

In the present study, we investigated the role of Cdc42 in JE-1 cells using ML141, a selective small-molecule inhibitor of Cdc42. We focused on alterations in epithelial permeability and the expression of genes related to inflammation and cell adhesion. Clarifying the mechanisms by which Cdc42 regulates JE barrier function may provide fundamental insights into the breakdown of the periodontal seal during periodontitis and identify novel therapeutic targets for preserving periodontal health.

Materials and Methods

1. Cell culture and ML141 treatment

The murine JE cell line JE-1 (Showa Medical University School of Dentistry, Tokyo, Japan) established by Seki et al.[10] was cultured in CnT-Prime epithelial culture medium (CELLnTEC, Bern, Switzerland) supplemented with 1% penicillin-streptomycin (Gibco, Carlsbad, CA, USA) at 37°C in 5% CO_2 in accordance with standard protocols. At 80% confluence, the cells were detached from the culture dishes using TrypLE Express Enzyme (1×) (Gibco). The Cdc42 inhibitor ML141 (Sigma-Aldrich, St. Louis, MO, USA) was dissolved in dimethyl sulfoxide (DMSO) and diluted with CnT-Prime medium to the required experimental concentrations, ensuring the final DMSO concentration remained less than 1%. JE-1 cells were treated with ML141 after reaching confluence, and all subsequent assays were performed 24 h post-treatment.

2. Cell viability assay

Cell viability was assessed using the CytoSelect MTT Cell Proliferation Assay (Cell Biolabs, San Diego, CA, USA) according to the manufacturer's instructions. JE-1 cells were treated with 1% DMSO (vehicle control) or varying concentrations of ML141 (0, 1, 10, 20, 40 μM) for 24 h. The absorbance was measured at 490 nm using a microplate reader (Infinite F50 Plus; TECAN, Männedorf, Switzerland).

3. RNA extraction and real-time reverse-transcription polymerase chain reaction

Total RNA was extracted from JE-1 cells using the RNeasy Mini Kit Plus (QIAGEN, Hilden, Germany) according to the manufacturer's instructions. Complementary DNA (cDNA) synthesis was performed using the Transcriptor First Strand cDNA Synthesis kit (Roche, Basel, Switzerland) according to the manufacturer's instructions. A quantitative polymerase chain reaction (qPCR) assay was performed using the StepOne Real-Time PCR System (Thermo Fisher Scien-

tific, Waltham, MA, USA). TB Green Premix Ex Taq II (TaKaRa Bio, Shiga, Japan) was used for the qPCR reaction. Specific primer sets for interleukin (*Il*)-*1b*, *Il-6*, *Mmp12*, *Cldn1*, *Gja1*, *Itgb4*, *Dst*, *Col17a1*, *Dsp*, *Dsg3*, and glyceraldehyde-3-phosphate dehydrogenase (*Gapdh*), were obtained from TaKaRa Bio. The cDNA amplification conditions were as follows: 95℃ for 30 s, followed by 40 cycles at 95℃ for 5 s and 60℃ for 30 s. Melting curve analysis was performed to confirm the specificity of the primers. The housekeeping gene *Gapdh* was used as an internal control. Data were analyzed using the ΔΔCt method, which included a calibration for control values.

4. Cell permeability assay

A cell permeability assay was performed according to a previously reported method[11]. JE-1 cells were cultured on transwell inserts in 24-well plates (CORNING, Corning, NY, USA) and treated with ML141 for 24 h. To assess permeability, 4 kDa fluorescein isothiocyanate (FITC)-dextran was added to the apical compartment at a final concentration of 267 μg/mL. After 30-, 90-, and 180-min incubation periods, 110 μL of medium was extracted from the basal compartment and replaced with an equal volume of CnT-Prime. Samples were collected in 96-well microtiter plates for subsequent analysis. Fluorescence was measured at 520 nm using a microplate reader (SpectraMax M2e; Molecular Devices, San Jose, CA, USA), and the apparent permeability (papp) was calculated using the following equation:

$$papp\ (cm/s) = (\Delta Q/\Delta t)/(A \times C_0)$$

where $\Delta Q/\Delta t$ is the cumulative amount transported, A is the diffusion area of the monolayer, and C_0 is the initial concentration of the FITC-dextran in the apical compartment.

5. Statistical analysis

Data are presented as mean±standard deviation. Comparisons between two groups were performed using Student's *t*-test, while comparisons among multiple groups were analyzed using the Tukey-Kramer honestly significant difference test. A p-value＜0.05 was considered statistically significant.

Results

1. Effect of ML141 on JE-1 cell viability

To determine the optimal concentration of ML141 for functional assays, cell viability was evaluated. Treatment with 1% DMSO or 1 μM or 10 μM ML141 had no significant effect on JE-1 cell viability (Fig. 1). Consequently, 10 μM was selected as the maximum non-cytotoxic concentration for subsequent experiments.

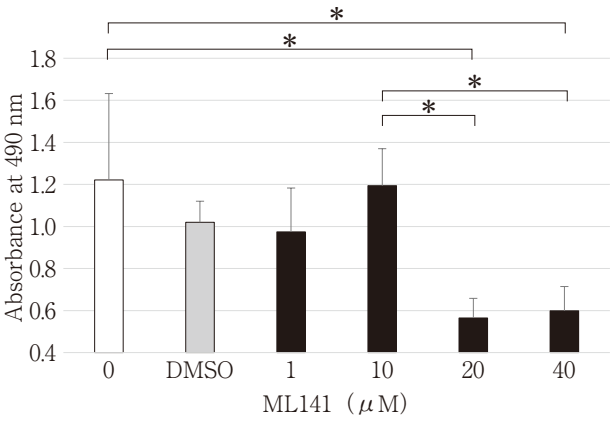

Fig. 1 Effect of ML141 on JE-1 cell viability
Cell viability was assessed using the CytoSelect MTT Cell Proliferation Assay. JE-1 cells were cultured with 1% DMSO, 0, 1, 10, 20, or 40 μM ML141 for 24 h. Optical density (OD) values at 490 nm are expressed. Data are presented as the mean±SD (n=6). *: p＜0.05 compared with the control (0 μM ML141). MTT, 3-(4,5-dimethylthiazol-2-yl)-2,5-diphenyltetrazolium bromide; DMSO, dimethyl sulfoxide; SD, standard deviation

2. Upregulation of inflammation-related genes in JE-1 cells after Cdc42 inhibition

qPCR analysis revealed that the inhibition of Cdc42 significantly altered the inflammatory profile of JE-1 cells. Treatment with 10 μM ML141 resulted in significant upregulation of the inflammatory mediators *Il1b*, *Il6*, and *Mmp12* compared with their levels in control cells (Fig. 2).

3. Effect of ML141 on the expression of cell adhesion molecules

To investigate the impact of Cdc42 inhibition on junctional integrity, we examined the expression of genes encoding key adhesion molecules. The expression level of *Cldn1*, a tight junction component, decreased markedly in JE-1 cells treated with 10 μM ML141 (Fig. 3A). Similarly, the expression level of *Gja1*, a gap junction component, decreased markedly in JE-1 cells treated with 10 μM ML141 (Fig. 3B). Additionally, the expression levels of *Itgb4*, *Dst*, *Col17a1*, *Dsp*, and *Dsg3*—hemidesmosomal and desmosomal components—were significantly reduced in JE-1 cells treated with 10 μM

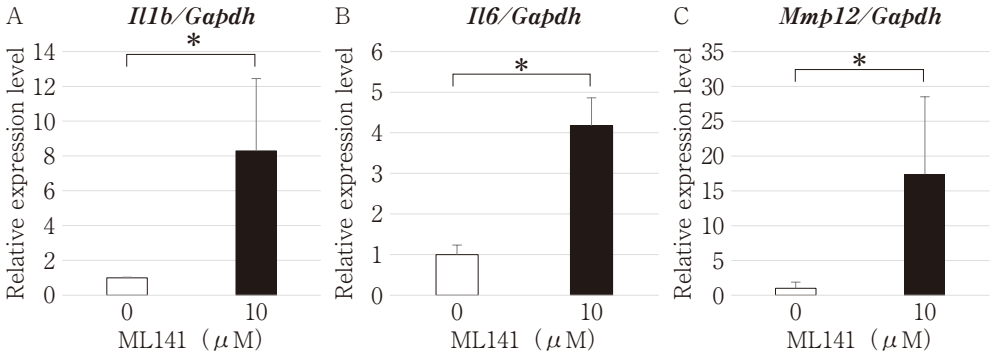

Fig. 2 Changes in inflammatory gene expression levels in JE-1 cells in response to ML141

Relative mRNA expression levels of (A) *Il1b*, (B) *Il6*, and (C) *Mmp12* in JE-1 cells treated with 0 or 10 μM ML141 for 24 h. Expression levels were normalized to *Gapdh*. Data are presented as the mean±SD (*Il1b*: n=3, *Il6*: n=3, *Mmp12*: n=6). *: $p<0.05$ compared with the control (0 μM ML141).

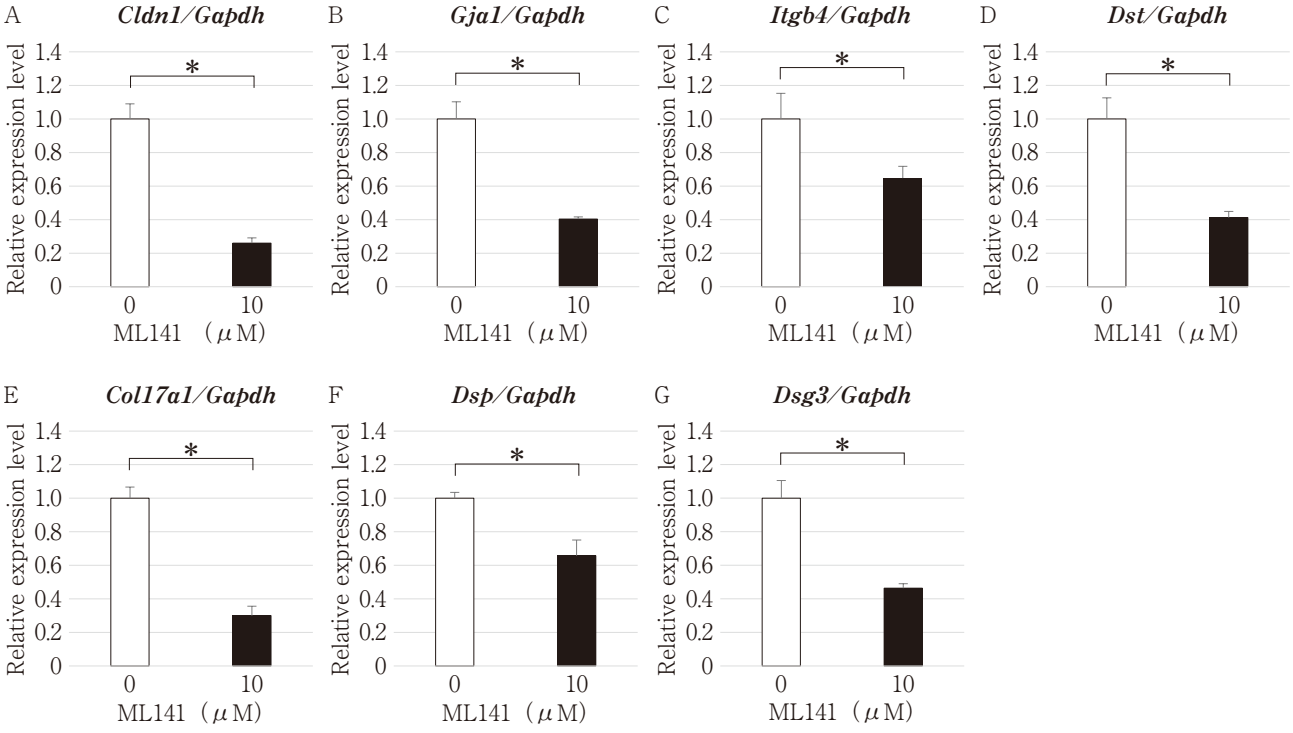

Fig. 3 Effect of ML141 on cell adhesion gene expression in JE-1 cells

Relative mRNA expression levels of (A) *Cldn1*, (B) *Gja1*, (C) *Itgb4*, (D) *Dst*, (E) *Col17a1*, (F) *Dsp*, and (G) *Dsg3* in JE-1 cells treated with 0 or 10 μM ML141 for 24 h. Expression levels were normalized to *Gapdh*. Data are presented as the mean±SD (n=6). *: $p<0.05$ compared with the control (0 μM ML141).

ML141 (Fig. 3C–G).

4. Cdc42 inhibition increased JE-1 epithelial permeability

Functional barrier integrity was assessed using a FITC-dextran permeability assay. JE-1 monolayers treated with 10 μM ML141 exhibited significantly increased permeability to FITC-dextran compared with control cells, indicating compromised epithelial barrier function (Fig. 4).

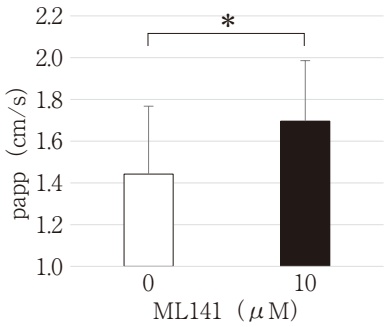

Fig. 4 Impact of ML141 on JE-1 intercellular permeability

Apparent permeability coefficient (papp) of FITC-dextran across JE-1 cell monolayers treated with 0 or 10 μM ML141 for 24 h. Data are presented as the mean± SD (n=6, *: $p<0.05$).

Discussion

In the present study, we investigated the effects of selective Cdc42 inhibition on the barrier function of JE-1 cells. Initial viability assays confirmed that ML141 at a concentration of 10 μM did not significantly affect JE-1 cell survival, whereas higher concentrations were cytotoxic (Fig. 1). This is consistent with previous studies on human immortalized gingival epithelial (HIGE) cells, where 10 μg/mL ML141 was effectively used to analyze Cdc42-dependent recycling pathways without compromising cell health[12]. Consequently, we determined that 10 μM represents an optimal concentration for assessing Cdc42 function, while excluding confounding cytotoxicity.

Inhibition of Cdc42 elicited a distinct inflammatory response in JE-1 cells, characterized by the significant upregulation of *Il1b*, *Il6*, and *Mmp12* (Fig. 2). *Il1b* is a potent initiator of the inflammatory cascade, often induced by noxious stimuli[13,14]. It is known to promote the expression of *Il6*, a pleiotropic cytokine that amplifies local inflammation[15]. Furthermore, inflammatory signaling can regulate *Mmp12*, a tissue-destructive enzyme that facilitates immune cell infiltration by degrading extracellular matrix components[16]. Mmp12 is a potent enzyme capable of degrading extracellular matrix components, and its overexpression accelerates tissue degradation and inflammatory cell infiltration in the pathogenesis of periodontal disease[17]. The pathophysiological significance of JE cells acquiring this destructive phenotype is profound; it suggests that during the progression of periodontitis, the epithelium itself autonomously drives the degradation of adjacent connective tissues, thereby directly contributing to chronic inflammation and irreversible periodontal destruction. The concurrent upregulation of these genes suggests that Cdc42 dysfunction triggers a signaling cascade that not only initiates inflammation, but may also promote tissue remodeling and periodontal destruction. Furthermore, the concurrent increase in the expression of *Il1b* and *Il6* alongside enhanced epithelial permeability highlights a potential vicious cycle linking inflammation and barrier dysfunction[18]. It is well-documented that pro-inflammatory cytokines such as IL-1β and IL-6 directly impair epithelial tight junctions and adherens junctions[19]. Therefore, the initial disruption of the junctional epithelial barrier caused by Cdc42 inhibition likely triggers the release of these cytokines, which in turn further dismantle intercellular adhesions and increase barrier permeability[18,19]. This self-reinforcing vicious cycle of continuous inflammation and progressive barrier breakdown has the potential to significantly accelerate the onset and progression of periodontal disease.

JE cells exhibit a distinctive molecular architecture across their primary junction types. Tight junctions contain occludin, multiple claudin isoforms (claudin-1, claudin-4, and claudin-15), scaffolding proteins (Zonula occludens-1 [ZO-1] and [ZO-2]), and junction adhesion molecule-A[20,21]. Gap junctions are formed by connexin 43 and connexin 26. Hemidesmosomes mediating tooth attachment comprise integrin $\alpha6\beta4$, laminin-5, BP180, BP230, and HD1 antigen, forming complexes in an epithelium-derived matrix lacking typical basement membrane components[22]. Desmosomes in the JE contain only desmoglein 3 (Dsg3), unlike oral and sulcular epithelia which express desmoglein 1 and 2[20]. In addition, *Dsg3* expression was observed in JE-1 cells. Regarding barrier structural integrity, ML141 treatment resulted in significant downregulation of *Cldn1*, *Gja1* (connexin 43), *Itgb4*, *Dst* (BP230), *Col17a1* (BP180), *Dsp*, and *Dsg3* expression levels (Fig. 3). These marked changes in intercellular adhesion factors suggest that intercellular adhesion was reduced by the inhibition of Cdc42. Given the unique attachment of the JE to the tooth surface mediated by hemidesmosomes, the downregulation of *Itgb4* and *Col17a1* is of paramount importance. The JE

binds firmly to the enamel and cementum via hemidesmosomes, providing a primary seal against bacterial invasion into the underlying periodontal tissues[23]. A reduction in core hemidesmosomal components, such as Itgb4 and Col17a1, signifies the structural failure of this epithelial-tooth mechanical adhesion. Consequently, this finding can be explicitly linked to "clinical attachment loss," a hallmark clinical phenomenon in chronic periodontitis characterized by the detachment of the junctional epithelium from the tooth surface, periodontal pocket formation, and the apical migration of the epithelium.

Intercellular adhesion structures, including desmosomes, serve as dynamic signaling platforms essential for maintaining epithelial stability and polarity[24–26]. Previous studies have shown that intercellular adhesion is critical for maintaining barrier function and that its disruption leads to increased permeability[27,28]. Our functional assays support this finding, demonstrating that Cdc42 inhibition significantly increased FITC-dextran permeability in JE-1 monolayers (Fig. 4).

Cdc42 has been shown to regulate intercellular adhesion molecules in epithelial cells via two distinct mechanisms. In the IQGAP1-mediated pathway, activated Cdc42 inhibits the dissociation of α-catenin from the cadherin-β-catenin complex by IQGAP1, thereby stabilizing the adhesion junction[29]. The other Par6-aPKC pathway plays a regulatory role in the stability of adherens junctions by controlling Arp2/3-dependent endocytosis[30]. It has been reported that constitutively activated Cdc42 induces the redistribution of several tight junction proteins, including occludin, ZO-1, claudin-1, claudin-2, and JAM-1[31]. It is thought that Cdc42 deficiency reduces the expression levels of these intercellular adhesion molecules. The observed decrease in the expression levels of intercellular adhesion molecules in the present study may have occurred through two mechanisms: direct disruption of cytoskeleton-dependent transcriptional networks and indirect suppression of adhesion molecules via inflammation-related signaling cascades. Specifically, Cdc42 acts as a critical regulator of actin dynamics, which directly influence mechanotransduction pathways such as the Yes-associated protein (YAP) and transcriptional coactivator with PDZ-binding motif (TAZ) signaling axis[32,33]. The inhibition of Cdc42 compromises actin polymerization, thereby potentially impairing the nuclear translocation and transcriptional activity of YAP/TAZ[32]. Because the YAP/TAZ mechanotransduction pathway is essential for the robust expression of adhesion-related genes and the maturation of cellular junctions[33], the disruption of this actin-dependent signaling axis provides a strong mechanistic basis for the extensive downregulation of adhesion mRNAs, including *Cldn1*, *Gja1*, *Itgb4*, and *Col17a1*, observed upon Cdc42 inhibition.

This study was based on gene expression and permeability analyses. Further research focusing on the subcellular localization of intercellular adhesion molecules and the structural integrity of intercellular junctions is necessary to definitively verify the adhesion dynamics in the JE. Furthermore, additional elucidation is necessary to determine the precise mechanism by which Cdc42 inhibition increases the expression levels of pro-inflammatory genes and suppresses the mRNA expression of various adhesion molecules, including intercellular junctions and hemidesmosomes.

Conclusions

In conclusion, the findings of the present study demonstrate that Cdc42 plays a critical role in maintaining the structural integrity and homeostasis of intercellular junctions in JE cells. Our observations revealed that pharmacological inhibition of Cdc42 in JE-1 cells led to impaired epithelial barrier function, as indicated by increased permeability, and induced an inflammatory response characterized by upregulation of *Il1b*, *Il6*, and *Mmp12*.

A notable observation was the significant decrease in the expression levels of intercellular adhesion molecules, which suggests that the loss of Cdc42 function affects intercellular adhesion structures. The results of this study indicate that Cdc42 plays a critical role in maintaining the tightness of the JE and that its dysfunction may contribute to the weakening of the epithelial barrier in periodontal tissues.

Funding

This study was supported in part by JSPS KAKENHI Grant Number JP23K09186 from the Japan Society for the Promotion of Science (Tokyo, Japan).

Acknowledgments

We would like to thank Editage (www.editage.jp) for

English language editing.

Conflicts of Interest

The authors declare that they have no conflicts of interest regarding this study.

References

1) Könönen E, Gursoy M, Gursoy UK. Periodontitis: A multifaceted disease of tooth-supporting tissues. J Clin Med 2019; 8: 1135.
2) Bhuyan R, Bhuyan SK, Mohanty JN, Das S, Juliana N, Juliana IF. Periodontitis and its inflammatory changes linked to various systemic diseases: A review of its underlying mechanisms. Biomedicines 2022; 10: 2659.
3) Nakamura M. Histological and immunological characteristics of the junctional epithelium. Jpn Dent Sci Rev 2018; 54: 59–65.
4) Demetriou NA, Ramfjord SP. Premitotic labeling and inflammation in the gingiva of Rhesus monkeys. J Periodontol 1972; 43: 606–613.
5) Bosshardt DD, Lang NP. The junctional epithelium: from health to disease. J Dent Res 2005; 84: 9–20.
6) Jiang Q, Yu Y, Ruan H, Luo Y, Guo X. Morphological and functional characteristics of human gingival junctional epithelium. BMC Oral Health 2014; 14: 30.
7) Bishop AL, Hall A. Rho GTPases and their effector proteins. Biochem J 2000; 348: 241–255.
8) Lee HK, Ji S, Park SJ, Choung HW, Choi Y, Lee HJ, Park SY, Park JC. Odontogenic ameloblast-associated protein (ODAM) mediates junctional epithelium attachment to teeth via tntegrin-ODAM-rho guanine nucleotide exchange factor 5 (ARHGEF5)-rhoA signaling. J Biol Chem 2015; 290: 14740–14753.
9) Zhang M, Wang X, Guo F, Jia Q, Liu N, Chen Y, Yan Y, Huang M, Tang H, Deng Y, Huang S, Zhou Z, Zhang L, Zhang L. Cdc42 deficiency leads to epidermal barrier dysfunction by regulating intercellular junctions and keratinization of epidermal cells during mouse skin development. Theranostics 2019; 9: 5065–5084.
10) Seki T, Aizawa R, Tanaka J, Yajima-Himuro S, Kato M, Tanaka K, Mishima K, Yamamoto M. Establishment of mouse gingival junctional epithelial cell line using a bioengineered tooth system. Biochem Biophys Res Commun 2018; 497: 167–172.
11) Aizawa R, Sunaga M, Tanaka K, Sugano M, Saito D, Okada K, Tanaka J, Mishima K, Yamamoto M. Effects of Porphyromonas gingivalis-derived lipopolysaccharide on the barrier function of cultured junctional epithelial cells. J Oral Biosci 2026; 68: 100721.
12) Takeuchi H, Takada A, Kuboniwa M, Amano A. Intracellular periodontal pathogen exploits recycling pathway to exit from infected cells. Cell Microbiol 2016; 18: 928–948.
13) Ren K, Torres R. Role of interleukin-1β during pain and inflammation. Biochem Pharmacol 2008; 60: 57–64.
14) Ford SG, Caswell P, Brough D, Seoane PI. The secretion of interleukin-1β. Cytokine Growth Factor Rev 2025; 84: 101–113.
15) Tanaka T, Narazaki M, Kishimoto T. IL-6 in inflammation, immunity, and disease. Cold Spring Harb Perspect Biol 2014; 6: a016295.
16) Shapiro SD, Senior RM. Matrix metalloproteinases. Matrix degradation and more. Am J Respir Cell Mol Biol 1999; 20: 1100–1102.
17) Lin B, Ser HL, Wang L, Li J, Chan KG, Lee LH, Tan LT. The emerging role of MMP12 in the oral environment. Int J Mol Sci 2023; 24: 4648.
18) Gao J, Cao B, Zhao R, Li H, Xu Q, Wei B. Critical signaling transduction pathways and intestinal barrier: implications for pathophysiology and therapeutics. Pharmaceuticals (Basel) 2023; 29: 1216.
19) Capaldo CT, Nusrat A. Cytokine regulation of tight junctions. Biochim Biophys Acta 2009; 1788: 864–871.
20) Hatakeyama S, Yaegashi T, Oikawa Y, Fujiwara H, Mikami T, Takeda Y, Satoh M. Expression pattern of adhesion molecules in junctional epithelium differs from that in other gingival epithelia. J Periodontal Res 2006; 41: 322–328.
21) Ye P, Yu H, Simonian M, Hunter N. Expression patterns of tight junction components induced by CD24 in an oral epithelial cell-culture model correlated to affected periodontal tissues. J Periodontal Res 2014; 49: 253–259.
22) Hormia M, Owaribe K, Virtanen I. The dento-epithelial junction: cell adhesion by type I hemidesmosomes in the absence of a true basal lamina. J Periodontol 2001; 72: 788–797.
23) Shimono M, Ishikawa T, Enokiya Y, Muramatsu T, Matsuzaka K, Inoue T, Abiko Y, Yamaza T, Kido MA, Tanaka T, Hashimoto S. Biological characteristics of the junctional epithelium. J Electron Microsc (Tokyo) 2003; 52: 627–639.
24) Schmidt A, Kaakinen M, Wenta T, Manninen A. Loss of $\alpha6\beta4$ integrin-mediated hemidesmosomes promotes prostate epithelial cell migration by stimulating focal adhesion dynamics. Front Cell Dev Biol 2022; 10: 886569.
25) Yang H, Xu Z, Peng Y, Wang J, Xiang Y. Integrin $\beta4$ as a potential diagnostic and therapeutic tumor marker. Biomolecules 2021; 11: 1197.
26) Borradori L, Sonnenberg A. Structure and function of hemidesmosomes: more than simple adhesion complexes. J Invest Dermatol 1999; 112: 411–418.

27) Varani J, McClintock SD, Aslam MN. Cell-matrix interactions contribute to barrier function in human colon organoids. Front Med (Lausanne) 2022; 9: 838975.
28) De Arcangelis A, Hamade H, Alpy F, Normand S, Bruyère E, Lefebvre O, Méchine-Neuville A, Siebert S, Pfister V, Lepage P, Laquerriere P, Dembele D, Delanoye-Crespin A, Rodius S, Robine S, Kedinger M, Van Seuningen I, Simon-Assmann P, Chamaillard M, Labouesse M, Georges-Labouesse E. Hemidesmosome integrity protects the colon against colitis and colorectal cancer. Gut 2017; 66: 1748–1760.
29) Fukata M, Kuroda S, Nakagawa M, Kawajiri A, Itoh N, Shoji I, Matsuura Y, Yonehara S, Fujisawa H, Kikuchi A, Kaibuchi K. Cdc42 and Rac1 regulate the interaction of IQGAP1 with beta-catenin. J Biol Chem 1999; 274: 26044–26050.
30) Georgiou M, Marinari E, Burden J, Baum B. Cdc42, Par6, and aPKC regulate Arp2/3-mediated endocytosis to control local adherens junction stability. Curr Biol 2008; 18: 1631–1638.
31) Bruewer M, Hopkins AM, Hobert ME, Nusrat A, Madara JL. RhoA, Rac1, and Cdc42 exert distinct effects on epithelial barrier via selective structural and biochemical modulation of junctional proteins and F-actin. Am J Physiol Cell Physiol 2004; 287: C327–335.
32) Mason DE, Collins JM, Dawahare JH, Nguyen TD, Lin Y, Voytik-Harbin SL, Zorlutuna P, Yoder MC, Boerckel JD. YAP and TAZ limit cytoskeletal and focal adhesion maturation to enable persistent cell motility. J Cell Biol 2019; 218: 1369–1389.
33) Panciera T, Azzolin L, Cordenonsi M, Piccolo S. Mechanobiology of YAP and TAZ in physiology and disease. Nat Rev Mol Cell Biol 2017; 18: 758–770.

Original Article

ODEP 6 (1) : 38～44, 2026

Effect of Light-irradiation Distance on the Bonding Performance to Root Canal Dentin Using a Dual-cure Composite Resin System

Asami YAMAMOTO, Yumika IDA, Tomoki IUCHI,
Kazuhide YONEKURA and Keiichi HOSAKA

Department of Conservative Dentistry, Tokushima University, Graduate School of Biomedical Sciences

Abstract

Purpose: To evaluate the effect of light-irradiation distance from the cementoenamel junction (CEJ) on the bonding performance of a dual-cure core build-up composite resin system to root canal dentin.

Methods: Twelve extracted human mandibular premolars were prepared with standardized post spaces (1.5×8 mm). A universal one-step adhesive (Clearfil Universal Bond Quick 2, UBQ2) and a dual-cure composite resin (Clearfil DC Core Automix ONE) were applied according to the manufacturers' instructions. Light curing was performed for 10 s at either 0 mm or 10 mm from the CEJ using an LED curing unit. The irradiance was 1,000 mW/cm^2 at 0 mm and 590 mW/cm^2 at 10 mm. After 24 h of water storage at 37°C, beam-shaped specimens (0.6×0.6 mm) were prepared and divided into coronal and apical groups. Micro-tensile bond strength (μTBS) was measured at a crosshead speed of 1 mm/min and statistically analyzed using Welch's *t*-test with Bonferroni correction. Failure modes were examined using scanning electron microscopy (SEM).

Results: The μTBS values were 29.8±8.7 MPa for coronal specimens at 0 mm and 15.1±5.1 MPa for apical specimens at 0 mm. At 10-mm irradiation distance, μTBS values were 16.3±5.8 MPa for coronal specimens and 12.1±5.5 MPa for apical specimens. A significant reduction in μTBS was observed in the coronal region when the irradiation distance increased from 0 mm to 10 mm ($p<0.05$). Additionally, at 0-mm irradiation distance, coronal μTBS was significantly higher than apical μTBS ($p<0.05$). SEM analysis showed less distinct adhesive interfaces and more interfacial defects in specimens cured at the longer irradiation distance.

Conclusion: Within the limitations of this study, increasing the light-irradiation distance significantly reduced bonding performance in the coronal region of root canal dentin, whereas apical bond strength remained consistently low regardless of irradiation distance. These findings suggest that reduced light availability may adversely affect bonding to root canal dentin; however, inadequate polymerization could not be directly confirmed because the degree of conversion was not measured. Optimization of curing protocols, solvent-evaporation strategies, and adhesive systems suitable for low-irradiance conditions may be necessary to improve bonding reliability in deep post spaces.

Key words: root canal dentin, light-curing distance, dual-cure composite, micro-tensile bond strength, adhesive dentistry

Corresponding author: Yumika IDA, Department of Conservative Dentistry, Tokushima University, Graduate School of Biomedical Sciences, 3-18-15, Kuramoto-cho, Tokushima 770-8504, Japan

TEL: +81-88-633-7340, E-mail: y-ida@tokushima-u.ac.jp

Received for Publication: April 15, 2026/Accepted for Publication: June 22, 2026

DOI: 10.11471/odep.2026-005

Introduction

Advancements in adhesive dentistry have enabled restorative procedures consistent with the principles of Minimal Intervention Dentistry (MID), which emphasize preservation of sound tooth structure and reinforcement of remaining tissues through durable adhesive interfaces.[1,2] Direct composite restorations supported by contemporary adhesive systems play a central role in this approach, allowing clinicians to achieve esthetic and functional outcomes while minimizing the removal of healthy tooth structure.[3]

In endodontically treated teeth, reliable bonding to root canal dentin is critical for retention of the core build-up and prevention of coronal leakage.[4] However, root canal dentin differs substantially from coronal dentin in both structure and composition. It exhibits fewer and narrower dentinal tubules, increased sclerosis, and reduced permeability, all of which hinder adhesive infiltration and limit the transmission of curing light.[5,6] Consequently, polymerization of adhesive systems and composite resins within the root canal is often incomplete.

In most *in vitro* studies, light curing is performed directly at the cementoenamel junction (CEJ), corresponding to 0-mm irradiation distance. Clinically, however, direct access to the CEJ is frequently restricted by adjacent teeth, root angulation, or limited interproximal space. Under such conditions, the light-curing unit must be positioned at a greater distance from the canal orifice, effectively increasing the irradiation distance. This geometric limitation markedly reduces the amount of light reaching the adhesive-dentin interface and may compromise polymerization efficiency.[7,8] Therefore, understanding the influence of irradiation distance is essential for achieving predictable bonding in deep and confined post spaces.

Light attenuation within the root canal further reduces polymerization potential. Irradiance decreases exponentially with distance and is additionally attenuated by absorption and scattering within dentin. Previous studies have reported reductions in irradiance of up to 70% at a depth of 10 mm, which correlate with decreased bond strength in apical regions.[9,10] Dual-cure adhesive and composite systems were developed to compensate for limited light transmission by incorporating chemically initiated polymerization. However, acidic environments can impair the amine-peroxide redox reaction, thereby limiting the effectiveness of chemical curing.[11]

In a previous study, a "touch-cure" mechanism was introduced to improve chemical compatibility between adhesive systems and dual-cure core build-up composites.[12] Although this approach enhanced overall bonding performance, bond strength in the apical region remained significantly lower than that in the coronal region, suggesting that optical factors such as irradiation distance continue to play a critical role.

Therefore, the aim of the present study was to evaluate the influence of light-irradiation distance on bonding performance to root canal dentin using a modern dual-cure core build-up system by analyzing micro-tensile bond strength (μTBS) and failure modes at coronal and apical levels.

The null hypothesis was that irradiation distance would not affect μTBS in either the coronal or apical regions.

Materials and Methods

1. Adhesive and composite systems

A one-step universal adhesive (Clearfil Universal Bond Quick 2, UBQ2, Kuraray Noritake Dental, Japan) and a dual-cure composite resin for core build-up (Clearfil DC Core Automix ONE, Kuraray Noritake Dental) were used (Table 1).

2. Specimen preparation

Twelve extracted human mandibular premolars were used in accordance with the Tokushima University Ethics Committee (Approval No. 4503). The teeth were allocated into two irradiation-distance groups: 0 mm and 10 mm, with six teeth in each group. After crown removal at the CEJ, standardized post spaces (1.5×8 mm) were prepared. Root canals were dried using endodontic suction and paper points, followed by application of the adhesive according to the manufacturer's instructions. Light irradiation was performed for 10 s using an LED curing unit (PenCure 2000, Morita, Japan) at either 0 mm (d=0) or 10 mm (d=10) from the CEJ. The irradiance of the curing unit was 1,000 mW/cm^2 at 0 mm and 590 mW/cm^2 at 10 mm. Radiant exposure was calculated by multiplying irradiance by irradiation time. For the adhesive, which was light-cured for 10 s,

Table 1 The compositions of the tested adhesive and resin composite

Materials	Manufacturer	Composition	Application protocol
Clearfil Universal Bond Quick 2 (UBQ2)	Kuraray Noritake Dental	10-MDP, Bis-GMA, HEMA, Hydrophilic amide monomer, Colloidal silica, Ethanol, DL-Camphorquinone, Accelerators, Water, Sodium fluoride	1. Apply BOND (Waiting time 0 s) 2. Dry with mild pressure air flow 3. Light-cure for 10 s
Clearfil DC Core Automix ONE		Silanated barium glass filler, Silanated silica, Bis-GMA, TEGDMA, DL-Camphorquinone, Chemical catalyst, Accelerators	Light cure of resin composite for 20 s

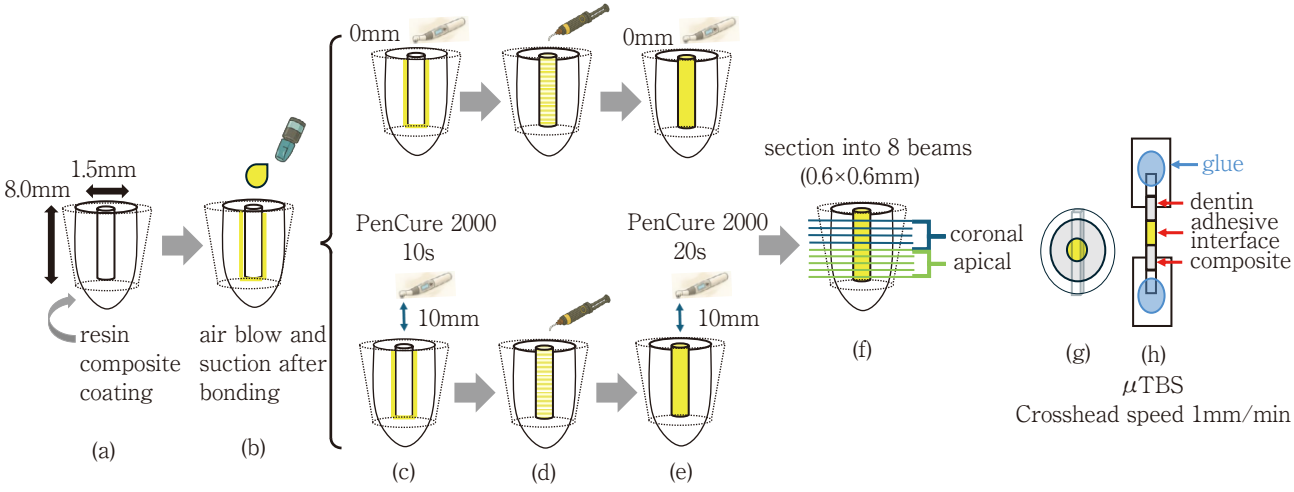

Fig. 1 Specimen preparation and sectioning of specimens for the micro-tensile bond strength test

(a) A post cavity of 8 mm depth and 1.5 mm diameter was prepared.

(b) All post cavities were dried with paper points and Clearfil Universal Bond Quick 2 was applied according to the manufacturer's instructions.

(c) Light irradiation was applied for 10 s using a PenCure 2000 LED unit (Morita) at either 0 mm (d=0) or 10 mm (d=10) distance.

(d) Post cavities were filled with a dual-cure composite resin (Clearfil DC Core Automix ONE).

(e) Light irradiation was applied for 20 s using a PenCure 2000 LED unit at either 0 mm (d=0) or 10 mm (d=10) distance.

(f) After 24-hour water storage, each root was cut into four slices of 0.6 mm thickness in both the coronal and apical regions.

(g) Each slice was cut centrally into a beam with a 0.6×0.6 mm surface area.

(h) Each beam was subjected to micro-tensile bond strength testing at a cross head speed of 1.0 mm/min.

the radiant exposure was 10 J/cm^2 at 0 mm and 5.9 J/cm^2 at 10 mm. For the resin core material, which was light-cured for 20 s, the radiant exposure was 20 J/cm^2 at 0 mm and 11.8 J/cm^2 at 10 mm. To minimize the influence of continuous use on light output, the light guide tip was cleaned before irradiation, and the curing unit was used under consistent conditions throughout the experiment. The same irradiation distance was maintained during adhesive application and subsequent core build-up procedures. The post spaces were filled with the dual-cure composite resin and light-cured for 20 s under the same conditions (Fig. 1).

3. Micro-tensile bond strength (μTBS) test

After 24 h of water storage at 37°C, specimens were sectioned perpendicular to the root axis into beam-shaped specimens with a cross-sectional area of 0.6×0.6

mm. From each tooth, four beams were prepared from the coronal region and four beams from the apical region, resulting in four experimental groups: [coronal (0)],[apical (0)],[coronal (10)], and [apical (10)]. Therefore, the maximum theoretical number of beam specimens was 24 for each experimental group.

No specimen loss occurred during specimen preparation. Pre-test failures were defined as beam specimens that fractured before μTBS testing. Such specimens were recorded and excluded from μTBS calculation and statistical analysis. The μTBS test was performed at a crosshead speed of 1 mm/min.

4. Failure mode analysis

Fractured specimens were examined using scanning electron microscopy (SEM; JCM-5700, JEOL, Japan). Failure modes were classified as adhesive failure, cohesive failure within the adhesive layer, mixed failure, or cohesive failure within dentin, based on the predominant fracture pattern.

The fracture surfaces were classified into the following four categories:

(A) Adhesive failure: Defined where ≥80% of the total fracture surface shows separation at the interface between the adhesive layer and dentin.

(Ca) Cohesive failure within the adhesive: Defined where ≥80% of the fracture surface exhibits cohesive separation within the adhesive (bonding) layer.

(M) Mixed failure: Assigned where no single failure mode accounts for ≥80% of the fracture surface, indicating a combination of adhesive and cohesive characteristics.

(Cd) Cohesive failure within dentin: Defined where ≥ 80% of the fracture surface shows cohesive separation within the dentin substrate or within the composite resin.

5. Statistical analysis

Normality was assessed using the Shapiro-Wilk test, and homogeneity of variance was evaluated using Levene's test. Because multiple beams were obtained from the same tooth, the tooth was considered the experimental unit. For each tooth, the μTBS values of beams obtained from the same region were averaged, and these tooth-level mean values were used for statistical analysis. Thus, the sample size for statistical analysis was six teeth per irradiation-distance group ($n=6$). Because heterogeneity of variance was detected, μTBS values were compared using Welch's *t*-test with Bonferroni correction. The level of significance was set at $p<0.05$.

Results

No specimen loss occurred during specimen preparation. Pre-test failures were observed only in the 10-mm irradiation group: two beams in the coronal region and two beams in the apical region. These specimens were excluded from μTBS calculation and statistical analysis. Specimens that yielded measurable μTBS values during tensile testing, even when the values were extremely low, were included in the statistical analysis. Accordingly, the final numbers of analyzed beams were 24 for [coronal (0)], 24 for [apical (0)], 22 for [coronal (10)], and 22 for [apical (10)].

For statistical analysis, the μTBS values of beams obtained from the same region of each tooth were averaged, and tooth-level mean values were used.

The data in all groups were normally distributed ($p>0.05$), while variances were not homogeneous ($p<0.05$). A significant reduction in μTBS was observed between coronal specimens cured at 0 mm and those cured at 10 mm ($p<0.05$). Additionally, at 0-mm irradiation distance, μTBS was significantly higher in the coronal region than in the apical region ($p<0.05$). No significant differences were detected between apical groups (Table 2).

SEM observations revealed well-defined adhesive layers and predominantly mixed failure patterns in coronal specimens cured at 0 mm. In contrast, specimens cured at 10-mm irradiation distance exhibited poorly defined adhesive interfaces and a higher incidence of interfacial failures, suggesting the presence of interfacial imperfections, such as gaps or voids (Fig. 2 and 3).

Discussion

The present study demonstrated that increasing the light-irradiation distance from 0 mm to 10 mm significantly reduced coronal μTBS, whereas apical μTBS remained consistently low regardless of irradiation distance. The irradiance of the curing unit was 1,000 mW/cm^2 at 0 mm and 590 mW/cm^2 at 10 mm, corresponding to radiant exposures of 10 and 5.9 J/cm^2 for the adhesive and 20 and 11.8 J/cm^2 for the resin core material, respectively. These findings suggest that reduced

Table 2 Micro-tensile bond strength (μTBS)

Group	μTBS
[coronal (0)]	29.8±8.7[a]
[apical (0)]	15.1±5.1[b]
[coronal (10)]	16.3±5.8[b]
[apical (10)]	12.1±5.5[b]

Values are mean±S.D.(MPa). Different lowercase letters indicate statistically significant differences among groups ($p<0.05$).

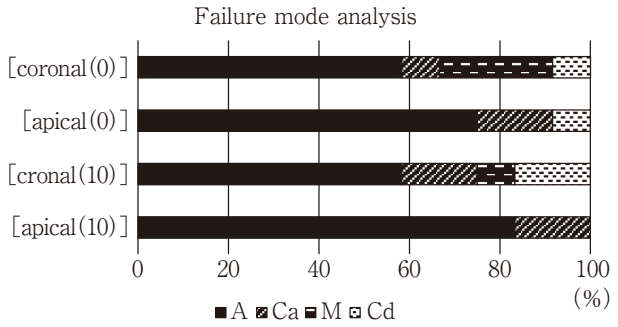

Fig. 2 Distribution of failure modes at the coronal and apical regions of post spaces

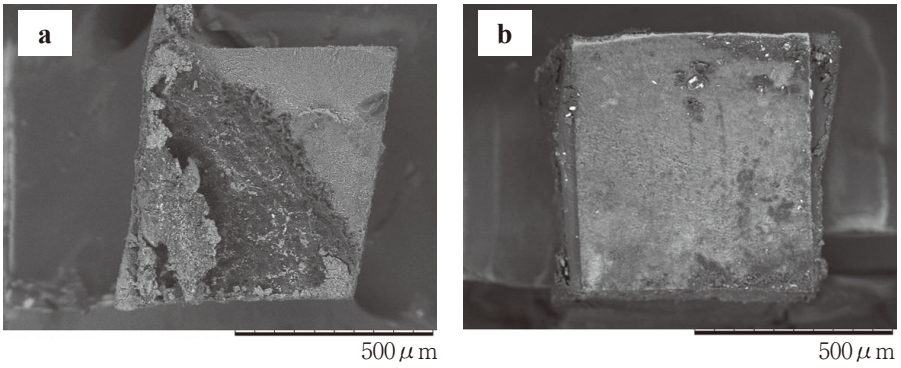

Fig. 3 SEM images of the adhesive interface in root canal dentin
(a) shows mixed failure in [coronal (0)], and (b) shows interfacial failure in [coronal (10)].

light availability at an increased irradiation distance may have contributed to the decrease in μTBS. However, because the degree of conversion was not directly measured in the present study, the reduction in μTBS should not be attributed solely to inadequate polymerization.

Polymerization of light-activated adhesives depends on absorption of blue light by camphorquinone and subsequent interaction with tertiary amines to generate free radicals. As irradiation distance increases, irradiance decreases and may be further attenuated by scattering and absorption within dentin. Our previous studies have consistently reported reduced bond strength to root canal dentin in deeper regions, particularly toward the apex, which may be associated with insufficient light transmission and reduced polymerization efficiency.[12,13] Recent evidence further suggests that increased curing distance and aging synergistically reduce bond strength in root dentin, especially when universal adhesives are used.[14] The significant reduction in coronal μTBS observed at 10-mm irradiation distance in the present study is consistent with these findings.

Dual-cure systems were developed to compensate for limited light transmission by incorporating chemically activated polymerization. However, chemical curing is known to be compromised in acidic environments, where protonation of tertiary amines suppresses the peroxide-amine redox reaction.[11,15] As a result, chemical activation alone cannot fully compensate for insufficient light curing, particularly in simplified adhesive systems. Although prolonged photo-irradiation has been reported to improve bonding performance to root canal dentin, especially in apical regions,[16] its effectiveness remains limited by anatomical and optical constraints.

Bonding to root canal dentin is further complicated by substrate-related factors. Compared with coronal dentin, root canal dentin—especially in the apical region—exhibits fewer and narrower dentinal tubules, increased sclerosis, and reduced permeability, all of which hinder adhesive infiltration and hybrid layer formation.[13,17] In addition, the cylindrical geometry of the

root canal results in a high configuration factor (C-factor), which amplifies polymerization shrinkage stress. If polymerization is compromised, this stress may exceed the developing bond strength and contribute to interfacial debonding.[18] Limited solvent evaporation in the confined canal space may leave residual solvent or water within the adhesive layer, potentially affecting monomer conversion, polymer cross-linking, and interfacial integrity.[19,20]

The relatively large standard deviation observed in the coronal (0) group may reflect specimen-to-specimen variability under favorable irradiation conditions. At 0 mm, sufficient light availability may have allowed some specimens to achieve relatively high μTBS values, whereas specimens affected by local interfacial defects, variations in adhesive thickness, solvent evaporation, or root canal morphology may have shown lower values.[6,17,21] This wider distribution of values may have contributed to the larger standard deviation in this group.

SEM observations in the present study supported the presence of interfacial differences among the experimental groups. Specimens cured at 0 mm exhibited more distinct adhesive interfaces, whereas those cured at 10 mm showed poorly organized interfacial features and a greater incidence of interfacial failures. These findings suggest the presence of interfacial imperfections, such as gaps or voids, in the long-distance irradiation group. However, SEM observations alone cannot directly demonstrate insufficient polymerization or reduced degree of conversion.

A methodological limitation of the present study is that the μTBS test specimens did not have a perfectly flat adhesive interface. Because the adhesive interface followed the curved root canal wall, uniform tensile stress may not have been applied to the entire bonded interface during loading. In addition, slight variations in the relationship among the specimen long axis, adhesive interface, and loading axis may have generated complex stresses, including bending, shear, and peeling stresses. Therefore, the μTBS values obtained in this study should be interpreted as apparent fracture resistance or relative comparative values under the present experimental conditions rather than as true tensile bond strength.[17,22]

Several limitations should be considered when interpreting the present findings. Although irradiance and radiant exposure were determined at each irradiation distance, the degree of conversion of the adhesive and resin core material was not directly measured. Therefore, the relationship between light attenuation, polymerization behavior, and bond strength could not be fully clarified. In addition, factors specific to the intracanal environment, including limited solvent evaporation, adhesive pooling, void formation, regional differences in root canal dentin, and high C-factor configuration, may have contributed to the reduced μTBS values, particularly in the apical region.[17,19,21]

Clinically, direct placement of the curing tip at the CEJ is often impractical. Under such conditions, clinicians may rely heavily on the chemical curing component of dual-cure systems. However, the present results indicate that this strategy alone does not ensure adequate bonding to root canal dentin. Improved outcomes may require a combination of optimized irradiation protocols, enhanced solvent evaporation techniques, and improved light-delivery strategies such as light-transmitting posts.

The null hypothesis was partially rejected, as irradiation distance significantly affected μTBS in the coronal region but not in the apical region.

Conclusion

Bond strength to root canal dentin decreased significantly with increasing light-irradiation distance in the coronal region, whereas apical bond strength remained consistently low regardless of irradiation distance. These findings suggest that reduced light availability may adversely affect bonding performance in root canal dentin. In addition to light attenuation, anatomical and environmental factors within the root canal, such as regional differences in dentin structure and limited solvent evaporation, may also contribute to the reduced bond strength, particularly in the apical region. Further optimization of curing protocols, solvent-evaporation strategies, and adhesive systems suitable for low-irradiance conditions may be necessary to improve bonding in deep post spaces.

Conflict of Interest

The authors declare no conflicts of interest associated with this manuscript, and consent has been obtained from the patient for the publication of the material.

Acknowledgments

The authors would like to express their sincere gratitude to Dr Masatoshi Nakajima for his valuable advice on this study. The authors also gratefully acknowledge Professor Kenichi Hamada and Dr Kazumitsu Sekine for their helpful advice regarding SEM observation.

References

1) Smales R, Yip K. Oral diagnosis and treatment planning: part 8. Reviews and maintenance of restorations. Br Dent J 2012; 213: 387–394.
2) Banerjee A, Frencken JE, Schwendicke F, Innes NPT. Contemporary operative caries management. consensus recommendations on minimally invasive caries removal. Br Dent J 2017; 223: 215–222.
3) Shu X, Mai QQ, Blatz M, Price R, Wang XD, Zhao K. Direct and indirect restorations for endodontically treated teeth. J Adhes Dent 2018; 20: 183–194.
4) Maruoka R, Nikaido T, Ikeda M, Ishizuka T, Foxton RM, Tagami J. Coronal leakage inhibition in endodontically treated teeth using resin-coating technique. Dent Mater J 2006; 25: 97–103.
5) Aksornmuang J, Nakajima M, Panyayong W, Tagami J. Effects of photocuring strategy on bonding of dual-cure one-step self-etch adhesive to root canal dentin. Dent Mater J 2009; 28: 133–141.
6) Thitthaweerat S, Nakajima M, Foxton RM, Tagami J. Effect of solvent evaporation strategies on regional bond strength of one-step self-etch adhesives to root canal dentine. Int Endod J 2013; 46: 1023–1031.
7) Taguchi K, Hosaka K, Ikeda M, Kishikawa R, Foxton RM, Nakajima M, Tagami J. The effect of warm air-blowing on the microtensile bond strength of one-step self-etch adhesives to root canal dentin. J Prosthodont Res 2018; 62: 330–336.
8) El-Askary FS, Van Noort R. Effect of air-drying pressure and distance on microtensile bond strength of a self-etching adhesive. J Adhes Dent 2011; 13: 147–153.
9) Foxton RM, Nakajima M, Tagami J, Miura H. Bonding of photo and dual-cure adhesives to root canal dentin. Oper Dent 2003; 28: 543–551.
10) Aksornmuang J, Nakajima M, Foxton RM, Tagami J. Mechanical properties and bond strength of dual-cure resin composites to root canal dentin. Dent Mater 2007; 23: 226–234.
11) Tay FR, Pashley DH, Yiu CK, Sanares AM, Wei SH. Factors contributing to the incompatibility between simplified-step adhesives and chemically-cured or dual-cured composites. Part I. Single-step self-etching adhesive. J Adhes Dent 2003; 5: 27–40.
12) Hosaka K, Yonekura K, Taguchi K, Tichy A, Kuno Y, Araoka D, Hatayama T, Sato K, Takahashi M, Nishitani Y, Ikeda M, Nakajima M, Tagami J. The influence of a Touch-cure System on the micro-tensile bond strength of self-etch adhesives to root canal dentin. Jpn J Conserv Dent 2019; 62: 39–46.
13) Kanno T, Ogata M, Foxton RM, Nakajima M, Tagami J, Miura H. Microtensile bond strength of dual-cure resin cement to root canal dentin with different curing strategies. Dent Mater J 2004; 23: 550–556.
14) Ismail HS, Ali AI, Elawsya ME. Influence of curing mode and aging on the bonding performance of universal adhesives in coronal and root dentin. BMC Oral Health 2024; 24: 1188.
15) Thitthaweerat S, Nakajima M, Foxton RM, Tagami J. Effect of waiting interval on chemical activation mode of dual-cure one-step self-etching adhesives on bonding to root canal dentin. J Dent 2012; 40: 1109–1118.
16) Aksornmuang J, Nakajima M, Foxton RM, Tagami J. Effect of prolonged photo-irradiation time of three self-etch systems on the bonding to root canal dentine. J Dent 2006; 34: 389–397.
17) Bouillaguet S, Troesch S, Wataha JC, Krejci I, Meyer JM, Pashley DH. Microtensile bond strength between adhesive cements and root canal dentin. Dent Mater 2003; 19: 199–205.
18) Feilzer AJ, De Gee AJ, Davidson CL. Setting stress in composite resin in relation to configuration of the restoration. J Dent Res 1987; 66: 1636–1639.
19) Dwiandhany WS, Sanon K, Shimada Y, Abdou A. Effect of solvent evaporation and photo-irradiation strategy of contact-cure adhesive system on bonding to root canal. Odontology 2026; 114: 862–875.
20) Matsumoto M, Mine A, Miura J, Minamino T, Iwashita T, Nakatani H, Nishida T, Takeshige F, Yatani H. Bonding effectiveness and multi-interfacial characterization of two direct buildup resin core systems bonded to post-space dentin. Clin Oral Investig 2017; 21: 309–317.
21) Alovisi M, Palopoli P, Comba A, Allais L, Roggia A, Baldi A, Pasqualini D, Berutti E, Scotti N. Morphological analysis and bond strength to root canal dentin of endodontically treated and retreated teeth: An ex vivo study. J Adhes Dent 2024; 26: 231–240.
22) Soares CJ, Soares PV, Santos-Filho PCF, Armstrong SR. Microtensile specimen attachment and shape—finite element analysis. J Dent Res 2008; 87: 89–93.

Submission Guidelines for *ODEP*

1. *ODEP* aims to develop conservative dentistry (operative dentistry, endodontology, and periodontology) through the publication of research and reviews on the following topics: (1) General dental medicine, clinical practice, and education on conservative dentistry; and (2) Conservative dentistry.
2. Papers are categorized into the following four types: (1) Original articles (reports on unique research discoveries); (2) Reviews (discussions on research questions and objectives to indicate future directions, or summaries of the contents of existing papers to propose new ideas); (3) Mini reviews (concise summaries of recent topics; mini reviews include papers awarded with prizes); and (4) Case and clinical reports (analysis of clinical records useful for dental care practice and development of the field of conservative dentistry). Reviews and mini reviews are categorized into the following: (1) Papers requested by the editorial board; and (2) Submitted papers.
3. Original articles and case and clinical reports are limited to the following: (1) Papers that have not been published in other journals; (2) Papers that are not presently submitted to another journal; and (3) Papers that are not presently scheduled for publication.
4. Acceptance or rejection of papers is determined through peer review (except for papers requested by the editorial board).
5. Submitted papers should be concisely written in English.
6. In principle, original articles should be organized as follows: (1) Abstract; (2) Introduction; (3) Materials and Methods; (4) Results; (5) Discussion; (6) Conclusion; (7) References; (8) Figure legend; (9) Figures and Tables. In principle, papers other than original articles should conform to the style format of original articles.
7. In principle, *ODEP* is published twice a year in June and December. In addition, special issues are published when appropriate.
8. The Japanese Society of Conservative Dentistry provides a certain amount of support for the listing fees of papers. For cases in which the lead author is not a member of the Japanese Society of Conservative Dentistry, such support is not provided. For cases in which the lead author is a member, but the co-authors include a non-member, partial support is provided. The cost to be borne by the authors is determined based on the number of non-members. The costs for figures, tables and photographs, for dispatching and offprints, and for creating the J-STAGE registration data are borne by the authors. In the case of papers requested by the editorial board, such costs are exempted.
9. Date of submission is the date when the submitted manuscript arrives at the secretariat of the Japanese Society of Conservative Dentistry. Date of acceptance is the date when the reviewers determine that the submitted manuscript can be published.
10. The listing order is the order of acceptance. A certification of publication will be issued upon request.
11. Manuscripts are to be submitted via the Japanese Society of Conservative Dentistry's website, e-mail, or postal mail. Manuscripts submitted for publication should be addressed to the secretariat of the Japanese Society of Conservative Dentistry.
12. In principle, authors can proofread their manuscript a maximum of two times. Extensive changes, additions, or deletions made to the contents of the manuscript cannot be accepted. Proofs should be returned by the designated date. If the authors do not need to proofread their manuscript, they should mention this on the left side of the cover page.
13. The copyrights for articles published in *ODEP* belong to the Japanese Society of Conservative Dentistry.
14. Matters not mentioned in these guidelines will be independently determined by the editorial board.
15. Authors' final manuscripts or publisher's versions (PDF) may be registered in the institutional repository from the time of electronic publication of the issue. The source must be indicated.

Submission of your manuscript for publication must conform to the following "Submission Guidance" as well as "Submission Guidelines."

The publishing charge is 10,000 yen for a Journal page including tables and figures. Extra charges for such as figures and tables preparation, color printing of photographs will also be paid by the authors. If authors do not pay publishing charge, the article may be retracted.

Submission Guidance (applied as of the Issue 1 of Vol. 4)

Manuscript organization

1. In principle, original articles should be organized into the following sections: (1) cover page; (2) abstract; (3) Main text (Introduction, Materials and Methods, Results, Discussion, and Conclusion); (4) References; and (5) Figure and table captions. Page numbering should start with the cover page. In principle, manuscripts, such as reviews or case reports, other than original articles should be organized in the same format as that of original articles.
2. Manuscript sections
   1) Title: The title should concisely describe the contents of the manuscript. The subtitle should also clearly describe the contents, and should not consist of only numbers.
   2) Introduction: The introduction should clearly describe the background, novelty, purpose, and significance of the study.
   3) Materials and Methods: This section should provide detailed information on the materials, equipment, or methods used along with clear instructions so that the experiments can be reproduced by others. Parameter settings, number of specimens, extraction methods, statistics processing, and others should comply with the purpose of the study.
   4) Results: This section should simply present the findings without bias or interpretation. Measurement results should show characteristic values including mean values and standard deviations.
   5) Discussion: This section should carefully consider the materials and methods, results, and others referring to relevant literature. Please note that it should not be overly assertive and should avoid off-topic points. The discussion should stay focused on the study purpose and not digress into a general discussion.
   6) Conclusion: The section should precisely summarize the results obtained and relate them to the purpose of the study and hypothesis as presented in the Introduction.
3. Manuscripts should be prepared using A4-size paper. The suggested length of each typed page is 80 alphanumeric characters per line×25 lines per page using a 12-point font. Top/bottom/left/right margins should be approximately 25 mm. Non-Japanese names and places should be in their original names.
4. For the manuscript style, refer to the latest issue of the journal.

Ethics code

1. Each report on the result of clinical research (clinical trial or observational research) or research involving any specimen collected from a human body must include a clear statement that it was approved by the head of the affiliated institution or by the research ethics review board assigned by the institution's head, in order to expressly indicate that the research was conducted in compliance with all applicable guidelines and laws, including the Declaration of Helsinki and the medical research guidelines, etc. issued by the Ministry of Health, Labour and Welfare including the following:
   1) Ethical Guidelines for Life Science and Medical Research Involving Human Subjects;
   2) Guidelines for Gene Therapy and Other Clinical Research; and
   3) Clinical Trials Act.
2. Each report on the result of research on, or a case concerning, regenerative medicine technology, etc. as defined

in the Act on the Safety of Regenerative Medicine must include a clear statement that the technology was provided to the patients in compliance with the aforementioned Act.

3. Each report on a case of a therapeutic method involving any off-label drug or device, or any pharmaceutical, medical device, regenerative medicine, or other related product not domestically approved must include a clear statement that the use was approved by the committee concerned (research ethics review board, review board for unapproved new drugs, etc.)at the affiliated institution or that the case report was approved for publication by *ODEP's* Clinical and Epidemiological Ethics Committee.
4. In each instance of publication of an academic paper, all personal information must be thoroughly protected so that none of the research subjects (patients) can be identified from it.
5. In each instance where a patient's clinical photo or X-ray image is included in an academic paper for publication, a clear statement must be provided that the consent of each such patient (or a parent, guardian, or proxy if the patient is a minor or in case it is otherwise difficult to obtain consent from the patient) was duly obtained.
6. Each report on the result of research involving animal subjects must include a clear statement that the research was approved by the animal experiment committee, etc. at the affiliated institution.

Cover page

1. The title, authors' names, institutional affiliations, and corresponding author's contact address should be centered, with a new line for each item, on the cover page.
2. The title should be in upper and lowercase letters, where the first letter of each word is uppercased and the remaining letters are lowercased. Articles, prepositions, conjunctions, and commonly used technical terms are lowercased. For hyphenated compound words, the letters following the hyphen should be lowercased.
3. The corresponding author's contact details should include the following information: one author's name, institutional affiliation, postal address, telephone and fax numbers, and e-mail address.

Abstract

1. The abstract should be a maximum of 400 words organized into four sections with the following headings: Purpose, Methods, Results, and Conclusion. Approximately three keywords should be placed at the end of the abstract.
2. Contributors should put considerable effort into preparing the abstract as it may determine whether or not the reader continues with the manuscript. When necessary, abstracts should be checked by a native English reviewer (preferably with expertise in dental medicine).

Main text

1. Introduction, Materials and Methods, Results, Discussion, and Conclusion are the main headings and are not numbered.
2. Subparagraphs should be numbered in the following order: 1. 2. 3. …; 1) 2) 3) …; (1) (2) (3) …; ① ② ③ …; and a. b. c. …
3. English characters should be written in the following manner:
   1) Generally, only the last name should be used to indicate a person.
   2) When the name of a product or manufacturer must be in the original language, the first letter of each word should be uppercased and the remaining letters lowercased.
      In principle, "generic name (product name, company name, city [state in the case of U.S.], country)"should be used in English manuscripts. Trademark and registration symbols ® and ™ are not required.
   3) Regarding common nouns in German or Latin, the first letter should be uppercased and the remaining letters lowercased. For common nouns in English and French, all letters should be lowercased.
   4) Regarding binominal nomenclature, the first letter of the genus should be uppercased and the remaining letters lowercased. The names of all genera and species should be italicized. When the same genus

appears frequently, it is acceptable to replace the name with the initial after the first use.

Example: *Streptococcus mutans* → *S. mutans*

5) For nouns that must be in their original language, other than German, Latin, English or French, all letters should be lowercased, except for commonly used technical terms.

4. In principle, SI units are used for measurements.
5. Any conflicts of interests (COI) must be declared after the conclusions. When there is no COI, the statement "The authors declare no conflict of interest related to this paper" should be included.
6. Acknowledgments for all sources supporting this study including grant funds should be added after of COI.

References

1. References must be listed at the end of the main text, and numbered in the same order as they appear in the text.
2. In the main text, a cited reference should appear with a superscript numeral and closing parenthesis. When two references are cited, a comma should be used to separate them; more than two references should be connected by an en dash between the first and last numeral.
   Examples: "by authors[3)]", "…is reported[7,8)]", "previous studies[10-15)]show"
3. Examples of Reference

a. Journal articles

Number) Last name and first name of all authors with a comma separating each author. Title of paper. Name of journal and publishing year in the Christian era; Volume number: Inclusive page numbers of paper.

Example:

1) Clark AB, Erickson D, Hamilton FG. Tensile bond strength and modulus of elasticity of several composite resins. J Dent Res 1992; 37: 618-621.

b. Book

Number) Author (co-authors). Title of book. First/last volume. Edition. Publisher's name: Publisher's location (City); Publishing year in the Christian era. Cited pages.

Example:

2) Phillips RW. Skinner's science of dental materials. 9th ed. WB Saunders: Philadelphia; 1991. 219-221.

c. Book with co-authors

Number) Contributor's name. Title of contributed article. Name of editor (editor-in-chief). Book title. First/last volume. Edition. Publisher's name: Publisher's location (City); Publishing year in the Christian era. Cited pages.

Example:

3) Torneck CD. Dentin-pulp complex. Ten Cate AR. Oral histology. 5th ed. Mosby: St. Louis; 1998. 150-196.

For cases in which each author's contribution is not separately indicated, the author's name and the title of the contributed article should not be listed.

Number) Name of editor (editor-in-chief). Title of book. First/last volume. Edition. Publisher's name: Publisher's location (City); Publishing year in the Christian era. Cited pages.

d. Other writing styles

・Abstracts of scientific meeting

Number) Presenter (all presenters should be cited. A comma should be used to separate the authors in the case of co-presentations.). Title of abstract. Name of journal and publishing year in the Christian era; Volume number: Inclusive page numbers, abstract number.

Example:

4) Marais JT. Cleaning efficacy of a new root canal irrigation material. J Dent Res 1998; 77: 669, Abst. No. 300.

・Journal articles in press

In principle, the same style as that of a regular journal article should be used; however, when the inclusive page

numbers are not known, they can be omitted. The statement "in press" should be shown at the end.

Example:

5) Sato K. Effect of toothbrushes on gingival abrasion. J Periodont Res 1994; 29: in press.

・Electronic journal

In principle, the same style as that of a regular journal article should be used; however, when the inclusive page numbers are not known, the DOI and other indicators should be shown. When papers are published in electronic journals before printing, the statement [Epub ahead of print] should be shown after the publishing year and month.

Example:

6) Sunada N, Ishii R, Shiratsuchi K, Shimizu Y, Tsubota K, Kurokawa H, Miyazaki M. Ultrasonic measurement of the effects of adhesive application and power density on the polymerization behavior of core build-up resins. Acta Odontol Scand; doi: 10.3109/00016357.2011.654252

・Internet website

Page publisher. Title of page. URL address. (Access date)

Example:

7) World Health Organization. Continuous improvement of oral health in the 21st century. http://www.who.int/oral_health/en/ (cited 2005. 10. 1)

4. In principle, journal names should be abbreviated in accordance with the format used by the journal.

Figures and tables

1. Figures, photographs, and tables are categorized into figures and tables, and then numbered. Paper size should be A4, and each figure and table should be printed on a separate page. The numbers allocated for the figures and tables should be consistent with those referred to in the text.
2. Figures and tables should be accompanied by explanations that are easily understandable. Explanations of figures/tables are presented as captions and explanations for tables/tables should be presented as footnotes.
3. If authors wish to have the figures shown in color, color data should be attached; if authors wish to have the figures shown in black and white, black-and-white data should be attached.

   Notes on creating imaging data:

   ・The jpg data format should be used if possible.

   ・Image size should correspond to the layout; image resolution should be at least 300 dpi for photographs and at least 1,200 dpi for line drawings.
4. If authors wish to reprint a figure from another publication, should be responsible for confirming whether permission is required from that publication, and obtaining permission if necessary. In addition, the source should be clearly stated in the explanatory text of each figure.

Sending manuscript intended for publication

1. The manuscript (cover page, abstract, main text, references, and figure and table captions are created as one file) should be formatted as a Microsoft Office Word (hereafter "Word") document.
2. Figures should be provided in jpg or pdf format.
3. Tables should be provided in Microsoft Office Excel, jpg, pdf, or Word format.
4. File titles should be as follows: "author name"_"university name (name after department is not needed)"_"manuscript/figure/table/submission form"_".filename extension (indicating file type)".

   Example) Nihon Tarou_Nihon University/manuscript.docx; Nihon Taro_Nihon University_Figure.jpg; Nihon Taro_Nihon Univesity_Table.xlsx; Nihon Taro_Nihon University_submission form.pdf

   Also, pdf files with embedded fonts for all contents are acceptable for submission. In such cases, file names should be as follows: Nihon Taro_Nihon University_comprehensive manuscript.pdf
5. E-mail title (subject) should be "Submitted papers for ODEP".

6. Submitted papers should be sent to the e-mail address of Oral Health Association of Japan: hensyu6@kokuhoken.or.jp. For safety, also send as a CC to hensyu5@kokuhoken.or.jp.
7. When e-mail submission is difficult for such reasons as the file size is too large, submission via an FTP server and other methods are acceptable. In such cases, the intent of submission should be informed by e-mail. In the e-mail, information regarding the site and other methods for downloading the file should be provided.
8. The submission form of *ODEP* provided on the Japanese Society of Conservative Dentistry's home page (https://www.kokuhoken.or.jp/form/ jscd/form-pub/) can be used for submission.

kuraray

Noritake

Super Low

1

Low

High

1色※で天然歯色に親和するフロアブルCR

※臼歯部の場合

クリアフィル®マジェスティ®ESフロー

Super Low　Low　High

Universal

なぜ色が親和するのか？ 物性は？ 操作性は？ 詳しい特長は特設サイトへ！ →

単品　クリアフィル® マジェスティ® ES フロー　Universal　管理医療機器 歯科充填用コンポジットレジン　医療機器認証番号：224ABBZX00170000

○本品は、袋包装です。

Super Low

●レジン充填材
〈Super Low〉（U、UD）各2.7g（1.5mL）
●付属品　ニードルチップ（N）(5個)
ニードルチップキャップ（5個）

Low

●レジン充填材
〈Low〉（U、UD、UOP、UW）各2.7g（1.5mL）
●付属品　ニードルチップ（N）(5個)
ニードルチップキャップ（5個）

High

●レジン充填材
〈High〉（U、UD、UOP）各2.7g（1.5mL）
●付属品　ニードルチップ（N）(5個)
ニードルチップキャップ（5個）

クラレノリタケ デンタル株式会社
〒100-0004　東京都千代田区大手町2丁目6-4 常盤橋タワー

お問い合わせ ｜ 0120-330-922 平日 10:00～17:00
ホームページ ｜ www.kuraraynoritake.jp

●仕様及び外観は、製品改良のため予告無く変更することがありますので、予めご了承ください。
●印刷のため実際の色調と異なる場合があります。
●ご使用に際しましては電子添文等を必ずお読みください。

［製造販売元］クラレノリタケデンタル株式会社　〒959-2653 新潟県胎内市倉敷町2-28
［販売元］株式会社モリタ　〒564-8650 大阪府吹田市垂水町3-33-18　お客様相談センター：0800-222-8020〈医療従事者様向窓口〉

03／2026

Thinking ahead. Focused on life.

MORITA

Spaceline EX

スペースライン EXが iFデザイン賞の金賞を受賞

ドイツのiFデザイン賞は、50年以上の歴史を有し、各国から選ばれた審査員によって厳正に選考される世界的に権威のあるデザイン賞です。世界中から6,400以上のエントリーが有った中、最優秀デザインとして75件に授与される金賞（ iF GOLD AWARD ）をスペースライン EXが受賞しました。人間工学に基づき緻密に計算されたデザインは、患者さんだけでなく術者にも理想的で洗練されたデザインであると評価されました。

iF GOLD AWARD 2018

発売

株式会社 モリタ

大阪本社　大阪府吹田市垂水町3-33-18
〒564-8650 T 06. 6380 2525
東京本社　東京都台東区上野2-11-15
〒110-8513 T 03. 3834 6161
お問合せ　お客様相談センター 歯科医療従事者様専用
T 0800. 222 8020（フリーコール）

製造販売・製造

株式会社 モリタ製作所

本社工場　京都府京都市伏見区東浜南町680
〒612-8533 TEL 075-611-2141
久御山工場　京都府久世郡久御山町市田新珠城190
〒613-0022 TEL 0774-43-7594

販売名：スペースライン
一般的名称：歯科用ユニット
機器の分類：管理医療機器（クラスⅡ）
特定保守管理医療機器
医療機器認証番号：228ACBZX00018000

www.dental-plaza.com

歯科接着用レジンセメント

Tokuyama

ESTECEM Ⅱ

BONDMER Lightless Ⅱで簡単前処理、術式の統一

BoSE Technology × Contact Cure

CR充填時のボンディング

支台築造時の前処理

補綴物・補綴装置の前処理

セメンティング時の前処理

補綴物も歯質も操作はひとつ

塗布後の待ち時間も光照射も不要！

エステセムⅡ

- CAD/CAMハイブリッドレジンも安定した接着力。
- 垂れにくく、余剰セメントも除去しやすいペースト。
- 無機フィラー74wt%で高強度を実現。

歯科接着用レジンセメント **エステセム Ⅱ** ボンドマー ライトレス Ⅱ セット （管理医療機器）認証番号228AFBZX00129000

オートミックスセット

標準医院価格 ￥20,500／セット

ハンドミックスセット

標準医院価格 ￥20,500／セット

詳細は特設サイトで！ https://www.tokuyama-dental.co.jp/bondmer2

株式会社トクヤマデンタル
本　社　〒110-0016 東京都台東区台東1-38-9
お問い合わせ・資料請求
インフォメーションサービス
0120-54-1182
受付時間
9:00～12:00/13:00～17:00（土日祝日は除く）

Webにもいろいろ情報載っています!!
トクヤマデンタル　検索

●札 幌 TEL011-812-5690　●仙 台 TEL022-717-6444　●東 京 TEL03-3835-7201　●名古屋 TEL052-932-6851　●大 阪 TEL06-6386-0700　●福 岡 TEL092-412-3240